FUNCTIONAL ORGANIZATION OF THE BED NUCLEUS OF THE STRIA TERMINALIS

by

Frank Nagy

A dissertation submitted to the

Graduate School-Newark

Rutgers, The State University of New Jersey

in partial fulfillment of requirements

for the degree of

Doctor of Philosophy

Graduate Program in Behavioral Neuroscience.

Written under the direction of

Professor Denis Paré

and approved by

_____

Eric Lang, PhD.

_____

Joan Morrell, PhD.

_____

Laszlo Zaborszky, MD.

_____

Denis Paré, PhD.

_____

Bart Krekelberg, PhD.

Newark, New Jersey

October, 2013

ABSTRACT OF THE DISSERTATION

Functional Organization of the Bed Nucleus of the Stria Terminalis

By Frank Nagy

Dissertation Director: Prof. Denis Paré

This thesis examined the functional organization of the bed nucleus of the stria terminalis (BNST), a poorly known brain region. Two series of experiments were performed. First, in anesthetized rats, we compared antidromic response latencies in anterior BNST (BNSTa) and central amygdala (CeA) neurons to brainstem stimuli. The frequency distribution of latencies was unimodal in BNSTa neurons (~10 ms) and bimodal in CeA cells (~10 and ~30 ms). After stria terminalis (ST) lesions, only short-latency antidromic responses were observed. Since BNST and CeA share excitatory basolateral amygdala (BL) inputs, lengthening the path of CeA axons might allow synchronization of BNSTa and CeA impulses to brainstem when activated by BL inputs. Consistent with this, the latency difference between CeA and BNSTa neurons to BL stimuli approximated that seen between the antidromic responses of BNSTa cells and CeA neurons with long-conduction times. These results point to a hitherto unsuspected level of temporal coordination between CeA and BNSTa neurons, supporting the idea of shared functions.

Second, in behaving rats, we recorded BNST neurons in anterolateral (BNST-AL) and anteromedial (BNST-AM) regions under spontaneous conditions

and during auditory fear conditioning. The firing rates of BNST- AL and AM neurons were highest in paradoxical sleep, lowest during slow-wave sleep and intermediate during wakefulness. During habituation, most neurons were unresponsive to the conditioned stimulus (CS). After fear conditioning, many BNST-AL neurons developed inhibitory responses to the CS whereas in BNST-AM, neurons with positive CS responses prevailed. The behavior of BNST-AM and AL neurons during contextual fear paralleled their CS responsiveness: BNST-AM neurons fired at higher rates during contextual freezing than movement whereas BNST-AL cells did the opposite. However, in contrast with cued fear where similar proportions of BNST- AM and AL neurons were CS responsive, many more BNST-AM than AL neurons showed differential activity in relation to contextual freezing. These findings point to regional differences in the activity of BNST-AL and AM in relation to learned fear, raising the possibility that they exert opposite influences on fear output networks. The stronger recruitment of BNST-AM neurons during contextual relative to cued fear may account for BNST's selective involvement in the former.

Acknowledgements

I would like to thank my advisor, Denis Paré, for his patience and dedicated mentorship during my PhD training. His insight, creativity, deep scientific knowledge and dedication to research has been an inspiration to me throughout my graduate career. I would also like to express my gratitude to the members of my committee: Bart Krekelberg, Eric Lang, Joan Morrell, and Laszlo Zaborszky for their support and critical analysis of my work. I am also indebted to Hreday Sapru, who gave me my start in neuroscience at UMDNJ while an undergraduate student. I would like to thank my colleague and fellow graduate student, Darrell Haufler, who taught me much about analysis and for his work in AIMS 2 & 3. It was a great pleasure to collaborate with him. My thanks and love extend to my two beautiful children, Rayan and Zain. Finally I would like to thank my mother, to whom this degree is dedicated. Words cannot express how much your love and support has meant to me.

Preface

The studies presented in Chapters IV and V are the result of a collaboration between myself and Darrell Haufler. A portion of this work is to be published in Learning and Memory.

TABLE OF CONTENTS

List of Figures

List of Abbreviations

AB:	accessory basal nucleus of the amygdala
BL:	basolateral nucleus of the amygdala
BLA:	basolateral complex of the amygdala (including BL, BM & LA)
BNST:	bed nucleus of the stria terminalis
BNSTa:	bed nucleus of the stria terminalis - anterior region
BNST-AL:	bed nucleus of the stria terminalis - anterolateral division
BNST-AM:	bed nucleus of the stria terminalis - anteromedial division
BNSTp:	bed nucleus of the stria terminalis - posterior division
CeA:	central amygdala
CeL:	lateral subdivision of the central nucleus of the amygdala
CeM:	medial subdivision of the central nucleus of the amygdala
CR:	conditioned response
CS:	conditioned stimulus
HPA:	hypothalamic-pituitary-adrenal
ITC:	intercalated nucleus
LFP:	local field potential
MeA:	medial amygdala
mPFC:	medial prefrontal cortex
NTS:	nucleus of the solitary tract
PAG:	periaqueductal gray
PTSD:	post-traumatic stress disorder

PVN:	paraventricular nucleus
RVLM:	rostro-ventrolateral medulla
ST:	stria terminalis
Str:	striatum
US:	unconditioned stimulus

CHAPTER I

INTRODUCTION

Hazardous, life-threatening events have always been a part of the world we live in. The dangers they contain may be real or perceived and present varying levels of threat to one's life. In the face of such conditions, an organism's survival depends on its ability learn the relationships between aversive events and the environmental stimuli that predict them. Emotions play a key role in this process by enhancing memory for these threats and the environments in which they occur. Indeed, the level of emotional arousal experienced can often predict how well an event will be remembered (McGaugh 2004). This key trait reveals an important function of the brain, namely the ability to prioritize incoming information with respect to the value it holds for survival. Emotions can subsequently rally immediate defense responses and help drive behaviors such as fight, flight and freezing. Taken together, these qualities have allowed fear to so serve as an important adaptive behavioral system essential to the survival of organisms throughout the animal kingdom. The occurrence of life-threatening, traumatic events can trigger the extreme end of this behavioral spectrum. These events may generate maladaptive responses in which fear becomes excessive, uncontrollable, and continues for an extended period after the threat has passed. These conditions may lead to anxiety disorders such as post-traumatic stress disorder. The mechanisms underlying fear learning and responses to fear are the subject of intense scientific scrutiny.

1.1) *Historical background*

In his book, The Expression of the Emotions in Man and Animals, Darwin

was one of the first to examine the role of emotions as they are translated into characteristic behavioral responses (Darwin 1872). In the process, he noted that many such behaviors are similarly expressed in various species, including humans. Darwin concluded that during the course of evolution, organisms acquired optimal response strategies that promote survival in the face of threatening stimuli. Such stimuli can induce a constellation of behavioral responses such as characteristic facial expressions, fight, flight and freezing. They also trigger autonomic and neuroendocrine system activity. These findings were the first to suggest that human emotion could be investigated through observations of animal behavior. The rise of experimental brain research in the 19th century focused on emotion as a key topic in this emergent field. With the help of Darwin's work, early scientists based their animal studies on the assumption that emotional circuits are conserved across species. Therefore, the study of non-human mammals might reveal key insights into the design and function of human emotional systems (reviewed by LeDoux 1987).

In subsequent years, observational experiments continued to discover the neurological underpinnings of fearful emotions. These studies initially focused on examining the effects of localized brain damage on emotional behavior. In an early study for instance, Brown & Schafer (1888) reported significant deficits in the emotional responses of monkeys with large temporal lobe lesions. Fifty years later, Kluver & Bucy elaborated on this effect. In an effort to understand the brain regions responsible for hallucinatory behavior under mescaline, they excised the medial temporal lobe of monkeys. The outcome of these surgeries was a

profound and unexpected effect on behavior. Among the cluster of behavioral changes exhibited following large temporal lobe lesions, monkeys were not able to recognize the emotional significance of objects nor the signals exchanged during social interactions (Kluver & Bucy, 1937). Subjects were also greatly muted in their own expression of fear and became tame. These behavioral effects became known as the Kluver-Bucy syndrome. Some twenty years later, Weiskrantz replicated the loss of fear in monkeys with Kluver-Bucy syndrome through more restricted lesions confined to the amygdala (Weiskrantz 1956). Weiskrantz singled out the amygdala as the structure responsible for associating affect with the sensory representation of an object. Research in this period also greatly benefited from the emergence and widespread use of behavioral models of emotional learning such a classical fear conditioning (Kellicut & Schwarzbaum 1963, Blanchard & Blanchard 1972, Kapp et al., 1979). The use of targeted lesions, emergent behavioral paradigms, and early electrical and chemical stimulation techniques (Maclean & Delgado 1953) served to create some of the initial conceptual models of limbic system architecture that underpin fear learning. These results lead researchers to agree that the amygdala serves as the hub of emotional processing in the brain.

1.2.1) *Pavlovian fear conditioning*

In the years since these seminal publications, many more studies have shown that the amygdala plays a key role in linking aversive stimuli to defensive behaviors (reviewed by Davis 2000; LeDoux 1998, 2000; Maren 2001, Paré

2004). The use of lesion techniques and the later advent of modern electrophysiological recording techniques contributed greatly to this understanding. However, perhaps the single greatest tool in the study of fear was the introduction of a behavioral paradigm called Pavlovian fear conditioning.

Developed by Ivan Pavlov in the early 1900's (Pavlov & Anrep 1927), Pavlovian (or classical) conditioning is perhaps the best known behavioral paradigm used to study learning and memory across a variety of brain systems and species (Krasne & Glanzman 1995, Holland & Gallagher 1999, Thompson & Krupa 1994). The past 30 years has seen a modified version of this behavioral model, known as Pavlovian *fear* conditioning, used to study the neurocircuitry supporting learned fear. In this variant, subjects are habituated to training and testing contexts and then presented with an innocuous conditioned stimulus (CS) – typically a tone, which is paired to an aversive unconditioned stimulus (US) – usually a footshock. The US reflexively activates an unconditioned response (UR). Even a single CS-US pairing is enough to form an associative memory between the two stimuli. The fear conditioning behavioral paradigm is summarized in Figure 1.1.

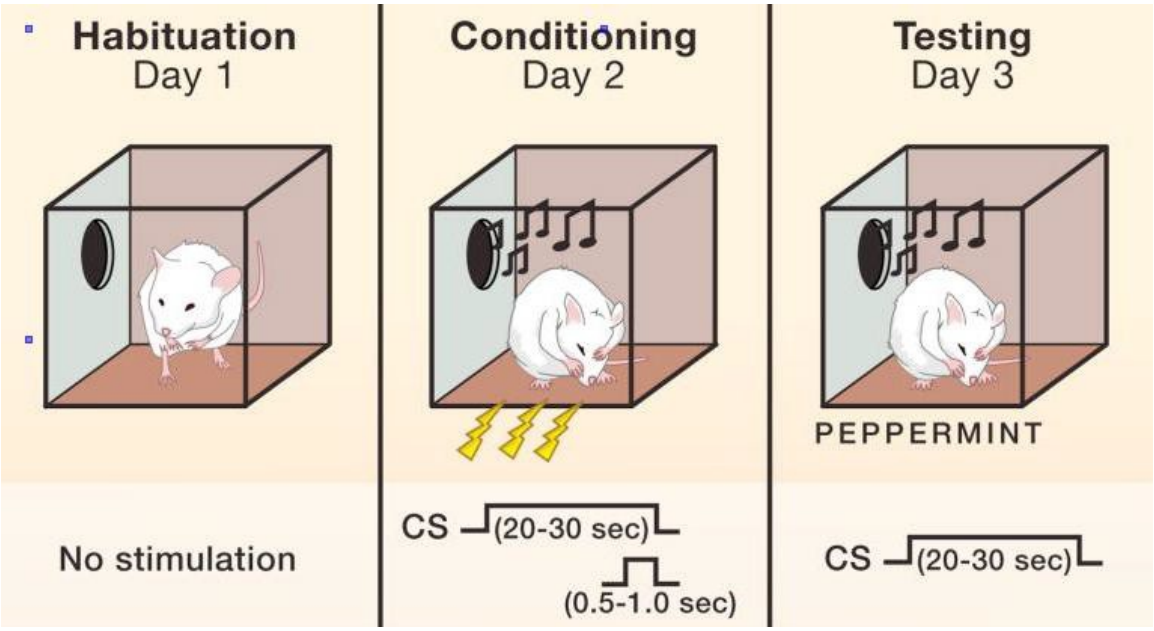

Fig. 1.1 Associative fear conditioning summary using tone-shock CS-US respectively (Adapted from Johannson et al. 2012). On Day 1, the subject is habituated to the conditioning chamber. On Day 2, a CS tone is presented and co-terminates with a short shock. Day 3 the CS tone is presented alone, in the absence of a shock. The grid floor is replaced with a peppermint coated flat floor to functionally change the environment. This is meant to allow the animal to freeze only to associate the CS and not the chamber to the fearful stimulus.

Once the memory is established, subsequent presentations of the CS alone evoke conditioned fear responses (CRs) identical to the US-evoked URs. Therefore the CRs become an index of the strength of the associative fear memory. Like URs, CRs are a combination of autonomic, neuroendocrine, and behavioral changes. Among these, the most commonly studied CRs include changes in heart rate, blood pressure, respiration (Kapp et al., 1979, Iwata et al., 1987), ultrasonic vocalization (Blanchard et al., 1991), behavioral freezing (Fanselow 1980), and escape behavior (Maier 1990). Pavlovian fear conditioning is a convenient behavioral paradigm used for the study of fear learning because memories are acquired rapidly and can last for the lifetime of the subjects (Gale

et al. 2004). Once established, these memories can be evoked by the presentation of the CS alone or by exposure to the context where training took place. However, if after conditioning the CS is repeatedly presented in the absence of a US, fear responses gradually disappear. This phenomenon is known as extinction.

Since the introduction of Pavlovian fear conditioning, enormous strides have been made in understanding the neural circuitry underlying fear learning in a variety of species, as summarized in the next section.

1.2.2) *The Amygdala and its role in fear learning*

The amygdala is composed of approximately twelve nuclei located in the temporal lobe. Although this thesis will focus on the amygdala's involvement in fearful emotions, it participates in numerous other functions. Indeed, animal studies have shown the amygdala to play key roles in reward learning (Will et al., 2004, Lu et al., 2005), the perception of painful stimuli (Kang et al., 1998), rage, arousal, feeding/drinking, and reproduction to name a few (Delgado 1968, Kaada 1972, Baxter & Murray 2002). Additionally, there are numerous fear related behaviors (innate fears, among others) that the amygdala does not participate in (Treit et al. 1993. Raybuck & Lattal 2011, Fendt 2003).

1.2.3) *Amygdalar anatomy*

The physician Karl Burdach was the first to describe the anatomical structure of the amygdala, referring to it as an almond-shaped nuclear complex in the anterior portion of the temporal lobe (Burdach 1819). His initial

characterization of the amygdala delineated a set of nuclei that would come to be known as the basolateral complex (BLA). Subsequent studies have expanded the description of the region to include the central (CeA), medial, and cortical nuclei (Sah et al., 2003, Ledoux 2000). These cell groups are further divided into subregions that maintain strong interconnections with one another. Several distinct nuclei within the amygdala play key roles in the acquisition and expression of fear memories (Fig 1.2). These include the BLA with its lateral (LA), basolateral (BL), and basomedial (BM) subdivisions, the CeA with medial (CeM) and lateral (CeL) subgroups, and the intercalated nuclei (ITC) (reviewed by Pape & Paré 2010). Within the amygdala, the synaptic connections are generally unidirectional. Neurons in the BLA send excitatory projections onto targets within the lateral and medial sector of the CeA. The ITC is able to modulate CeA firing via inhibitory projections to that cell group. The CeM meanwhile is thought to be the main output nuclei of the amygdala, projecting to regions mediating the expression of fear with its control over these areas modulated by BLA and ITC activity.

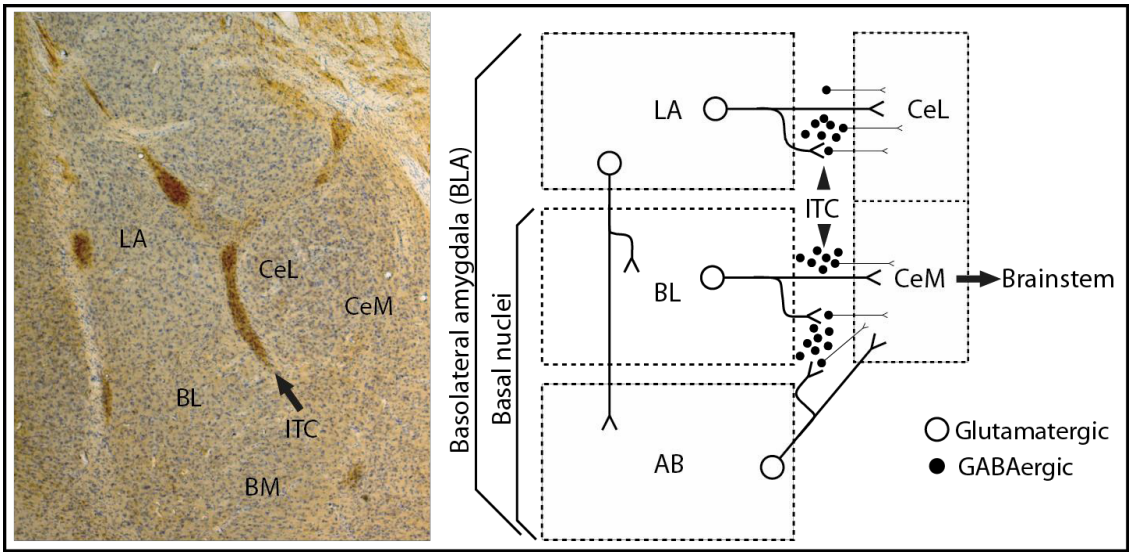

Fig. 1.2 (A) Section processed to reveal μOR immunoreactivity and counterstained with cresyl violet. (B) Box diagram showing main intra-amygdaloid projections. Note that all BLA projections to CE are glutamatergic. There are GABAergic neurons in BLA nuclei but they are local-circuit cells. BM, accessory basomedial nucleus; BL, basolateral nucleus; CeL and CeM, lateral and medial sectors of CeA; ITC, intercalated neurons; LA, lateral nucleus. OT, optic tract;

1.2.4) *Extrinsic Amygdalar Connectivity*

In addition to its extensive intrinsic connectivity, the BLA and CeA have abundant connections with many other regions of the brain (Fig. 1.3)

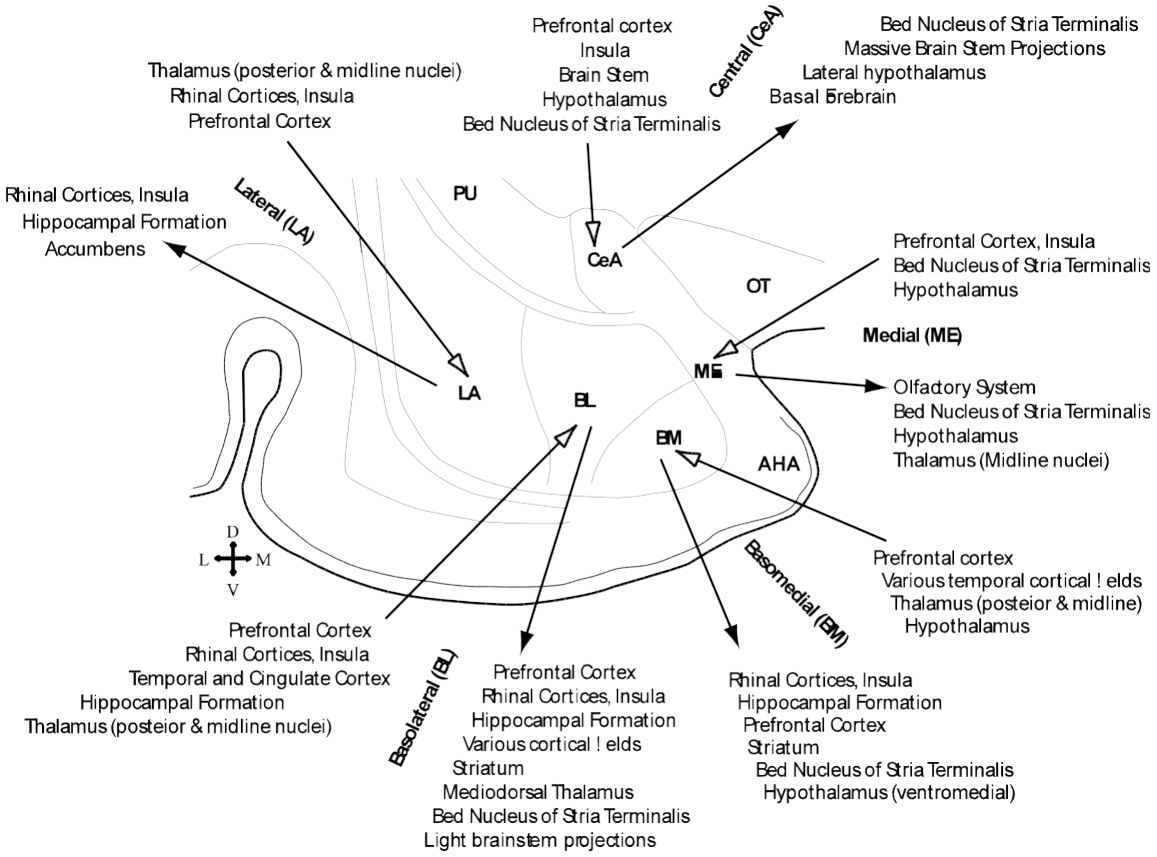

Fig. 1.3 Summary of the main connections of the amygdala. Note that for simplicity, inputs from and projections to neuromodulatory systems of the brainstem and basal forebrain have been omitted.

Via inputs from the thalamus, associative cortical areas, as well as more direct subcortical routes, the amygdala has access to sensory inputs of all modalities. The main input station of the amygdala for sensory information is the lateral nucleus (Amaral et al 1992, LeDoux et al. 1990a). The amygdala, particularly the BLA complex also receives inputs from the hippocampus (McDonald 1998). Hippocampal inputs can relay information regarding the environmental context of aversive events (Ji & Maren 2007). Additionally, polymodal cortical regions, particularly the medial prefrontal cortex, transmit highly processed information to the amygdala (McDonald 1998).

US-related shock information can reach the LA via its inputs from posterior intralaminar thalamic nuclei (Paré et al. 2004). The CeA also has direct, albeit sparse projections to the paraventricular nucleus of the hypothalamus (PVN), the entry point in the brain to the HPA axis (Guillemin and Rosenberg, 1955). The CeA, along with the BLA have much stronger projections to the BNST, a structure with more robust hypothalamic connectivity (Dong et al., 2001). The amydalar-BNST-hypothalamic circuit might be one possible route through which the amygdala could engage the stress circuitry during fear expression (Rogan & LeDoux ,1996; LeDoux, 2000).

1.2.5) *The Amygdala and conditioned fear*

Studies from numerous laboratories are in agreement that the amygdala plays a critical role in the acquisition and expression of conditioned fear (Davis, 2000; Ledoux, 2000; Maren 2001). The thalamus and cortex relay CS and US information that in turn converges on LA neurons. These inputs, when paired, lead to a potentiation of synapses conveying CS information to LA neurons (LeDoux, 2000; for review see Paré et Duvarci 2012). The LA can then indirectly drive CeM fear output neurons through its projections to BA, ITC and CeL nuclei (Pitkanen et al., 1997; Royer et al., 1999).

The CeA is thought to be the main output nucleus of the amygdala for the expression of conditioned fear responses. Damage to the CeA has been shown to severely reduce fear expression (Kapp et al., 1979; Iwata et al., 1986). The CeA is well positioned to elicit the complex autonomic neuroendocrine and

behavioral responses to fearful stimuli through its numerous projections to downstream targets such as the lateral hypothalamus, rostral ventrolateral medulla (RVLM), nucleus of the solitary tract (NTS) (Cassell and Gray 1989; Iwata et al., 1987;LeDoux et al. 1988; Hopkins and Holstege 1978), and periaqueductal gray (Carobrez et al., 1983).

1.2.6) *Measuring the expression of fear*

The subjective experience of emotions does not easily lend itself to scientific study. However, the behavioral and physiological correlates of emotions, especially fearful emotions, can be studied easily. In rats, fearful responses have been measured in a wide variety of ways, including behavioral freezing (Blanchard and Blanchard 1972; Ledoux et al., 1986), potentiated startle (Davis 1997), ultrasonic vocalizations (Blanchard et al., 1991), and changes in heart rate and blood pressure (Kapp et al., 1979). Of these, freezing is the easiest to measure (Kalin and Shelton 1989). Operationally, behavioral freezing is defined as the arrest of all movement other than breathing. In the wild, such behavior allows rats to remain inconspicuous, decreasing the likelihood of a predator attack (Biederman et al., 2001).

The periaqueductal gray (PAG) is not a storage site of classically conditioned fear associations, but an expression site of conditioned freezing (Wilson and Kapp 1994). Lesions of the PAG abolish freezing without affecting other components of fear responses (LeDoux et al., 1988). As a result of direct CeM projections, the PAG generates freezing responses to conditioned stimuli

(Rizvi et al., 1991; Hopkins & Holstege, 1978). The PAG also receives inputs from all portions of the BNST although the strongest arise from the ventral and posterior lateral divisions of the BNST - the same regions of the BNST that receive CeM projections (Dong & Swanson 2004, 2006a, b). Thus there seems to be a rich interplay among CeM, BNST, and PAG neurons for the purposes of driving fearful behaviors. The nature of these interactions, however, remains unclear. One of the goals of this thesis is to understand the timing of inputs from BNST and CeM neurons to downstream targets such as the PAG.

1.3.1) *BNST background*

The BNST was originally defined by JB Johnston as the mass of cells surrounding the fibers of the stria terminalis at its rostral and caudal ends. (Johnston 1923). On the basis of comparative and embryological studies, Johnston further proposed that the similarities between the CeA and BNST are so profound that they would be better classified as part of the same cell continuum. As a result of Johnston's early observations, the concept of the 'extended amygdala' was developed (Alheid et al., 1995; Alheid & Heimer 1988). These studies demonstrated that the CeA, the medial amygdala (MeA) and BNST were connected by columns of cells located along the trajectory of the stria terminalis – the fiber bundle that connects the amygdala with the BNST. In the ensuing decades anatomists have reclassified the boundaries of the BNST. The caudal end of Johnston's BNST became the CeA with a few cells around the caudal tip associated with the BNST. The rostral end however, has continued to

be thought of as the BNST and defined as the region surrounding the stria that is bounded by the lateral septal nucleus ventrally, the preoptic region of the hypothalamus dorsally, the amygdala caudally and the nucleus accumbens on its rostral end.

1.3.2) *Anatomy of the BNST*

At a macroscopic level, BNST can be divided into a posterior region (BNSTp) that is sexually dimorphic and involved in reproductive/defensive behaviors (Simerly 2002), and an anterior region (BNSTa). The BNSTa will be the focus of this thesis as it is most often implicated in the regulation of anxiety and contextual fear (Davis et al. 2010). As shown in figure 1.4, and consistent with earlier accounts (Krettek & Price ‘78), we divide BNSTa into three sectors: medial (BNST-AM) and a lateral sector (BNST-AL) – both dorsal to the anterior commissure, and a third sector (BNST-AV) – ventral to the anterior commisure. Figure 1.4 also shows how these regions differ in terms of inputs from the amygdala (Fig. 1.4C), cortex (Fig. 1.4D), as well as subcortical outputs (Fig 1.4E).

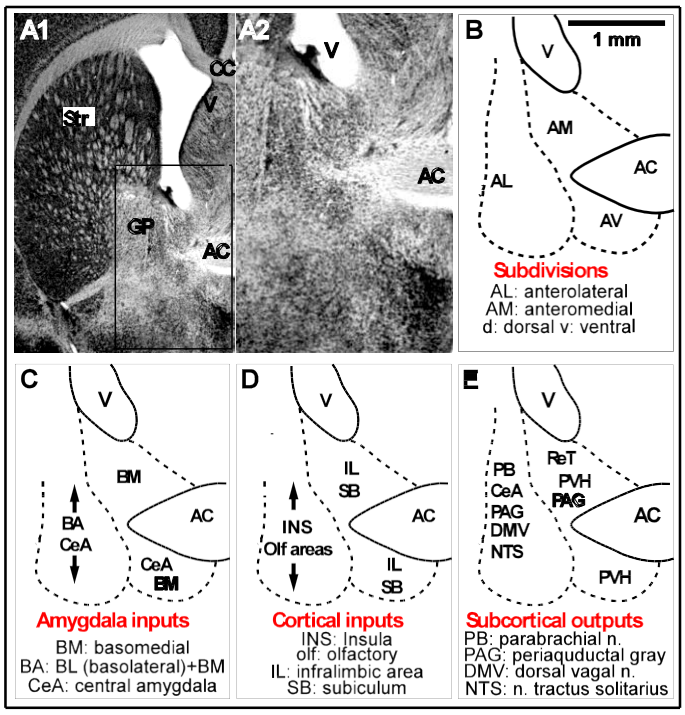

Fig 1.4 Structure and connections of BNSTa. (A) BNSTa at low (1) and higher (2) magnification. NeuN staining. (B) BNSTa subdivisions based on differential patterns of connectivity shown in panels C-E. (C) Amygdala inputs. (D) Cortical inputs. (E) Subcortical projections. Note that nearly all BNSTa projections to brainstem fear effectors (PAG, NTS, DMV) originate from the anterolateral region. The lateral and medial parts of BNST are also distinct in their cortical afferents. Differential amygdala innervation of the two regions has also been reported. Abbreviations: AC, anterior commissure; GP, globus pallidus; PVH, paraventricular hypothalamic nucleus; ReT, Reuniens thalamic nucleus; Str, striatum; V, ventricle.

1.3.3) *Connections of the BNST*

As mentioned before, the main extrinsic input to BNSTa originates from the amygdala (Fig. 1.4C; Krettek & Price 1978; Weller & Smith 1982; Dong et al., 2001a; Shin et al., 2008; Sun & Cassell 1993). Amygdalar inputs to BNSTa are important in the context of this thesis because they likely transfer CS information to BNSTa. Axons from the amygdala reach the BNST via two distinct pathways, the stria terminalis (dorsal pathway) and the ansa peduncularis (ventral pathway) (Dong et al. 2001a). From the amygdala, the BNSTa derives massive GABAergic

inputs that arise in CeA, and dense glutamatergic inputs that stem from the basal nuclei (BA = BL + BM; basolateral and basomedial respectively). CeA and BA inputs converge in the lateral part of BNSTa. Differentiated amygdala inputs are seen in the medial part of BNSTa (Fig. 1.4B). It is important to note that whereas the connections between BNSTa and the BA nuclei are largely unidirectional, BNSTa-CeA connections are reciprocal (Sun & Cassell 1993; Dong et al., 2001a; Poulin et al., 2006). Most brainstem projections of BNSTa, including those to the ventrolateral periaqueductal gray (PAGvl), originate in its lateral sector, with a small contribution from BNST-AM (see Schwaber et al., 1982; Sofroniew 1983; Luppi et al. 1988; Moga et al., 1989; Sun et al., 1994). Like the CeA, the BNSTa projects to a variety of structures thought to generate different components of fear responses including the PAGvl, nucleus tractus solitarius (NTS), and dorsal motor nucleus of the vagus nerve (DMV) (Dong et al., 2000; Dong et al., 2001b; Dong & Swanson 2004) . The BNST also sends massive projections to the hypothalamus, subserving its role as the conduit for limbic inputs regulating the HPA axis (Dong et al. 2000). BNSTa projections to the PAGvl (Hostege et al. ‘85) were reported to be stronger than those originating in CeM (Hopkins & Holstege ‘78) and are likely to underlie the influence of BNSTa over behavioral freezing.

1.3.4) *The BNST and its role in fear learning*

As previously mentioned, a large body of literature implicates the amygdala in Pavlovian fear conditioning. However, the transformation of fearful sensory cues into appropriate behavioral responses relies on the dynamic interaction of a distributed network of cell groups in multiple nuclei. It has been

shown that stimulus convergence in the thalamus (Gerren and Weinberger 1983) and auditory cortex (Lezkus et al 2011) are necessary for auditory fear-conditioning. The hippocampus and entorhinal cortex have been shown to be important in the context-dependence of fear (Ji & Maren 2007, Maren 2008). Lesioning and neuroimaging studies have also implicated the prefrontal cortex-amygdala circuit in the processing of fear conditioning and extinction (Bishop 2007, Quirk & Beer 2006).

While the BNST has similar cells types and projection patterns as the CeA, the notion that the BNST is involved in generating conditioned fear to discrete sensory cues is not supported by prior studies. Indeed it is generally believed that the CeA and BNST have different and independent functions (Walker et al., 2003; Davis et al. 2010). In particular, lesion (Hitchcock and Davis 1987, 1991; LeDoux et al. 1988; Campeau and Davis 1995) and local drug infusion studies (Kim et al. 1993; Wilensky et al. 2006) have revealed that CeA is critically involved in the rapid expression of conditioned fear responses to discrete sensory cues (however see Koo et al., 2004; Pitts et al., 2009). These functions are reportedly left intact by BNST lesions (LeDoux et al. 1988; Walker and Davis 1997; Gewirtz et al. 1998; Sullivan et al. 2004). Instead, BNST lesions were reported to interfere with the development of longer “anxiety-like” states in response to more diffuse environmental contingencies (reviewed in Walker et al. 2003; Davis et al. 2010). For instance, inactivation of BNST impairs light-enhanced startle whereas CeA inactivation does not (Walker & Davis 1997; Walker et al. 2003). Similarly, it was reported that post-training electrolytic lesions

of BNST disrupt corticosterone and freezing responses to contextual stimuli but not conditioned freezing to discrete sensory cues (Sullivan et al. 2004).

Given their common inputs from the basolateral amygdala and overlapping projections to fear effector neurons, the basis for the functional dissociation between BNST and CeA is unclear. However, other studies suggest that BNST activity, while not required for generating learned fear to cues, exerts a tonic inhibitory influence on fear output networks. For instance, intra-BNST infusions of muscimol enhance fear potentiated startle (Meloni et al., 2006). Moreover, presentation of a fear-eliciting CS together with a conditioned inhibitor can *increase* fos expression in BNST relative to animals only presented with the CS (Campeau et al., 1997). Thus, the question remains: What exactly is the BNST's role in the acquisition and expression of conditioned fear does in interact with the CeA during this process?

1.4.1) *Objectives and hypothesis*

Our current understanding of the BNST is reminiscent of the situation that prevailed 20 years ago for the amygdala. In the early 90's, the extrinsic connectivity of the amygdala was known and we had much lesion and pharmaco-behavioral data about its function. However, the amygdala was somewhat of a black box because there was little data about the activity of amygdala neurons in behaving animals. The same situation now exists for BNST. Therefore, we propose to use in BNST, the strategy that proved successful to reveal the inner workings of the amygdala.

The goals of this thesis are: (1) to expand our understanding of the relationship between the BNST and the amygdala; (2) to examine the behavior of BNST neurons under different states of vigilance, and (3) to characterize the behavior of BNSTa neurons during the acquisition and expression of conditioned fear responses.

In Chapter III for my first aim, I will examine the conduction times and trajectory of CeA and BNST outputs to the brainstem. As reviewed above, both these cell groups project to overlapping areas of the brainstem such as the nucleus of the solitary tract and the PAG, sites mediating central control of blood pressure and freezing behavior, respectively. Their postsynaptic impact on these regions could be enhanced if BNST and CeM impulses reached these targets at the same time. However, the conduction time of BNST and CeM neurons to the brainstem targets has yet to be characterized. Furthermore, it has previously been observed that some CeM neurons reach their brainstem targets directly, through the ventral amygdalofugal pathway whereas others take a much longer route through the stria terminalis (Price and Amaral, 1981). Thus, I will first aim to characterize the conduction time of CeM and BNST neurons to the brainstem. My hypothesis is that lengthening the path of the CeA axons to the brainstem via the stria terminalis can facilitate the synchronization of BNST and CeM impulses to the brainstem.

In Chapter IV for my second aim, I will study the spontaneous activity of BNST-A neurons during different behavioral states of vigilance. Because most

prior unit recording studies of BNST have been performed in anesthetized animals (for instance see Adamec, 1989; Yajeya et al., 1989; Han and Ju, 1990; Veinante and Freund-Mercier, 1998), there is little data on this topic. Here, we hypothesize that like most neurons of the central nervous system (reviewed in Steriade & Hobson, 1976), BNSTa neurons exhibit higher firing rates during activated behavioral states (wakefulness and paradoxical sleep) than slow-wave sleep.

Finally, in Chapter V, I examine the activity of BNSTa neurons during the acquisition and expression of cued and contextual fear. As reviewed above, prior work suggests that the CeA participates in the expression of cued and contextual fear whereas BNSTa is only involved in the latter. The basis for this functional dissociation is unclear because CeA and BNST form similar connections with the amygdala and brainstem fear effectors. To shed light on this question, we will record neurons in BNST-AL and AM in rats subjected to auditory fear conditioning. Because these two BNSTa sectors form contrasting connections with the amygdala and downstream targets, we hypothesize that that there will be regional differences in the activity of BNSTa neurons in relation to learned fear.

CHAPTER II

GENERAL METHODS

2.1) *Acute in vivo experiments*

Experiments were conducted on Male Sprague-Dawley rats (225-250 g; Charles River, Wilmington, MA), in accordance with the NIH Guide for the Care and Use of Laboratory animals and with the approval of the Institutional Animal Care and Use committee of Rutgers State University, in compliance with the Guide for the Care and Use of Laboratory Animals (Department of Health and Human Services). All animals were kept on a 12 hour light/dark cycle and had free access to food and water. Rats were anesthetized with a mixture of ambient air, oxygen, and isoflurane. Atropine (0.05 mg/kg, i.m.) was administered to aid breathing. Body temperature was maintained at 37-38 ^{o}C with a heating pad. The level of anesthesia was assessed by continuously monitoring the electroencephalogram and electrocardiogram. A local anesthetic (bupivacaine, 0.1 ml) was injected subcutaneously in the region of the scalp to be incised. Ten minutes later, the scalp was cut on the midline. The bone overlying the regions of interest was removed and the dura mater opened. Under stereotaxic guidance, groups of two or three tungsten stimulating electrodes (inter-tip spacing of ~1 mm) were inserted in the BL nucleus of the amygdala, the stria terminalis, as well as just dorsal to the substantia nigra where CeA and BNST axons en route to the brainstem form a compact bundle (Hopkins and Holstege 1978; Holstege et al. 1985). For the placement of stimulating and recording electrodes, the following stereotaxic coordinates were used (all relative to the bregma and in mm). For BL, antero-posterior (AP) – 2.3, medio-lateral (ML) 5.0, dorso-ventral (DV) 8.7, and

AP –2.8, ML 4.8, DV 8.7. For CeM, the coordinates were AP –2.6, ML 4.1, DV, 8.0 and AP –1.8, ML 3.6, DV 7.8. For BNST, the coordinates were AP –0.8. ML 1.7, DV 6-7.5 and –0.2, ML 1.6, DV 6-7.5. For brainstem, three electrodes were inserted at the same AP level (-6.0), three different ML levels ML 1.6, 2.1, 2.6, and DV positions 7.7, 7.3, 6.9, respectively.

Evoked responses were recorded in CeM and BNST with high impedance (10-12 Mohm) tungsten microelectrodes (FHC, Bowdoin, ME). The positions of the microelectrodes were adjusted independently with micromanipulators. A subset of rats was prepared with electrolytic lesions of the stria terminalis. Such lesions were performed by applying 1 mA for 10 seconds. We only considered neurons generating spikes with a high signal to noise ratio (>3). As the electrodes were lowered toward the structures of interest, electrical stimuli (0.1-0.5 mA, 0.1-0.3ms) were delivered in the brainstem in search of antidromically responsive neurons, indicating that they are brainstem-projecting cells. To be classified as antidromic, evoked unit responses had to meet at least two of the following three criteria (Lipski 1981): (1) stable latency (<0.3 ms jitter), (2) collision with orthodromically evoked or spontaneously occurring spikes and (3) ability to respond faithfully to high frequency stimuli (300 Hz). Neuronal activity was observed on a digital oscilloscope, digitized at 20 kHz, and stored on disk for off-line analysis.

At the end of experiments, the animals were administered an overdose of sodium pentobarbital (100 mg/kg, i.p.) and select recording sites in the BNST and CeM were marked with electrolytic lesions (0.6 mA for 5-10 s). The brains

were then extracted from the skull, fixed in 2% paraformaldehyde and 1% glutaraldehyde, sectioned on a vibrating microtome (thickness 100 um), and stained with cresyl violet to show electrode placements, as shown in figure 3.1. The microelectrode tracks were reconstructed by combining micrometer readings and histology. To be included in the analysis, cells had to be histologically confirmed as being located in the regions of interest. Analyses were performed off-line with commercial software (IGOR, WaveMetrics, Lake Oswego OR; Matlab, Natick, MA) and custom-designed software running on personal computers. Spikes were detected using a window discriminator after digital filtering of the raw waves. All values are expressed as means ± SE.

2.2) *Survival Surgeries*

These experiments involved the use of implanted microdrives housing multiple tetrodes. Recordings were made over the course of a week, during which rats were exposed to a differential fear conditioning paradigm.

2.2.1) *Surgical procedures*

Adult male Lewis rats (Charles River) were housed individually with *ad libitum* access to food and water and maintained on a 12 h light/dark cycle. Rats were anesthetized with a mixture of isoflurane and O_2, and administered atropine to aid breathing. In aseptic conditions, rats were mounted in a stereotaxic apparatus with nonpuncture ear bars. A local anesthetic (bupivacaine, s.c.) was injected into the region to be incised. The scalp was then incised and a craniotomy performed above the regions where electrodes were to be implanted.

Next, anchoring screws were secured to the skull around the exposed region. The microwire assembly was then lowered into position with the aid of a stereotaxic device. All exposed areas of the brain were sealed using an agar solution. The microdrive was then affixed to the skull using dental cement to securing it to the mounting screws. A reference screw was inserted in the bone overlying the cerebellum and soldered to the reference wire. The tetrodes were then individually lowered using the adjusting screws until they were in their regions of interest. The remaining wound was sutured and covered with antibiotic ointment. The rats were then allowed to recovery for 7 days before the start of the behavioral protocol.

2.2.2) *Microdrive Arrays*

Each micro-drive array houses 21 individually adjustable microdrives (Fig. 2.1). The original design of this array (Kloosterman et al., 2009) was modified by adjusting micro-drive angles and widening the base to facilitate the targeting of multiple brain regions. Tetrodes were gold-plated using a combined low impedance progressive plating process in the presence of a gold/carbon nanotube solution (CheapTubes, Battleboro VT) (Ferguson et al., 2009). The solution was continuously sonicated during the plating process to promote greater adhesion of the gold mixture (Desai et al., 2010). Plating was performed using multiple rounds of low current until electrode impedance is lowered to ~100 kOhms. Electrode interface boards were custom designed to match the micro drive dimensions (Advanced Circuits, Tempe AZ). Boards were then connected to

Plexon preamplifiers (Neuralynx, Bozeman, MT). Reference channels on electrode interface board were attached to stainless steel reference wires originating from screws above the cerebellum.

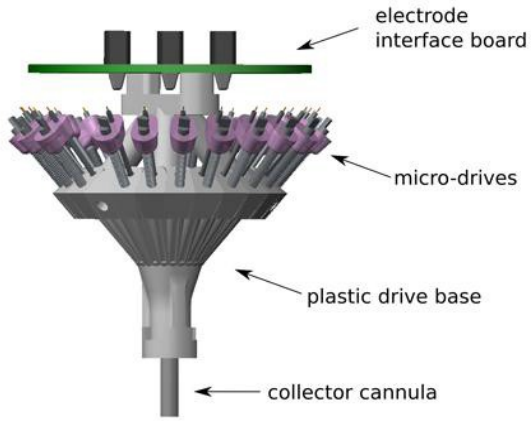

Fig. 2.1 Model of micro-drive array. Tetrodes are pinned to the outer edge of the electrode interface board which then attaches to 16 channel preamplifiers. The plastic array consists of 21 micro-drives, each driving one tetrode. The collector cannula region was modified in-house to accommodate a wider range of recording sites (not shown).

2.3) *Fear Conditioning*

On day-0, rats were habituated to context A and B for 20 min each. Before and after each context exposure, the animals were placed in their home cage. On day-1, we performed a tone habituation session (5 presentations of the CS^+ and the CS^-; each 30 s in duration, white-noise or 2 kHz, 80 dB). The identity of the CS^+ and CS^- was varied across animals and they were presented in a random order. The CS^- served as non-associative control. Following habituation, the rats received presentations of 5 CS^+ and 5 CS^-, with the CS^+ co-terminating with a footshock (US, 0.5 mA, 1s). On day-2, to test for contextual fear memory, rats were placed in context A for 10 min with no presentations of the CS^+ or CS^-.

On day-3, in context B, recall of cued fear was tested with twenty additional presentations of the CS^- and CS^+. Another recall test was performed on day-4 (ten additional presentations of the CS^+ and CS^-). In all phases, five minutes elapsed between placement of the rats in context A or B and presentation of the first CS. The duration of the CS was always 30 sec and the inter-CS intervals varied between 3 and 4 minutes. This long interval was selected so that during the recall tests, freezing elicited by one CS would have subsided by the time the next CS is presented. However, note that during fear conditioning, once the first US was administered, rats froze at various times, including during the CSs and inter-CS intervals. Much of this freezing likely represents a non-associative response to the recent US exposure. Behavior was recorded by a video-camera and scored off-line. Time spent freezing (defined as immobility, with the exception of breathing) was measured by an experienced observer with a stopwatch. Contextual freezing was also measured using a custom Matlab script that compared absolute differences in luminosity values between corresponding pixels in successive video frames. Prior to carrying out this analysis, the frames were filtered with a two-dimensional median base filter to remove the so-called “salt-and-pepper” noise in luminosity values of nearby pixels. We used a uniform threshold of luminosity variations (10% of maximal seen during locomotor activity) that had to be observed in at least 30 consecutive frames (or 1 sec). This automated approach closely matched the results obtained with visual scoring ($r = 0.9$).

2.2.4) *Statistical analyses*

To assess whether CS-evoked responses were significant, we first computed the firing rate of each unit in 5 sec bins, from 20 s before to 120 s after the onset of the CS^+ and CS^-. Separate averages were obtained for the habituation phase, the first two and last three CS^+ and CS^- of training, as well as the first and last five CS^+ and CS^- of the two recall tests. The data of each average was then z-scored to firing rate variations seen in the pre-CS period. A CS-evoked change in firing rate was deemed significant, when the six 5-s bins of the CS^+ or CS^- differed from the baseline period by ±1.96 z or more. This corresponds to a significance threshold of $p \leq 0.05$. To assess whether the proportion of responsive cells changed significantly depending on the phase of the behavioral protocol, we used a chi-square test that analyze whether there was a dependence between response type (response, no response) and behavioral phase (habituation, CS^+ 1-2 or 3-5 of training, first 5 or last 5 CS^+ of the two recall tests.

2.2.5) *Histology*

At the end of the experiments, the animals were deeply anesthetized and recording sites marked with small electrolytic lesions (20 µA between a tetrode channel and the animals' tail for 15 sec). One day later, the rats were then perfused-fixed through the heart, their brains extracted, cut on a vibrating microtome and the sections counterstained with cresyl violet.

CHAPTER III

AIM #1

TIMING OF IMPULSES FROM THE CENTRAL AMYGDALA AND BED NUCLEUS OF THE STRIA TERMINALIS TO THE BRAIN STEM

3.1) *Rationale*

The CeM and BNST possess remarkable anatomical, embryological, and neurochemical similarities. As a result they have been grouped together by Alheid and Heimer in an inclusive structure termed the 'extended amygdala'. Furthermore, the two structures are reciprocally connected through the ventral amygdalofugal pathway and stria terminalis, potentially allowing them to modulate each others' activity. Functionally however, the two nuclei are quite different. The CeM is thought to be the main amygdalar output driving the expression of rapid responses to discrete fearful stimuli. The BNST in contrast mediates longer lasting behavioral responses to less defined contingencies. Both nuclei carry out at least a portion of their respective behavioral influences through their connections to similar brainstem regions. To gain a greater understanding of functional interactions between these two structures, we compared the antidromic response latencies of BNST and CeM neurons to brainstem stimulation. While BNST neurons exhibited a frequency distribution of latencies that was unimodal (~10 ms mode), CeM neurons had a bimodal distribution (~10 and 30 ms modes). Because a subset of brainstem projecting neurons in the CeM course through the stria terminalis, we examined the effect of stria terminalis lesions on the frequency distribution of CeM neurons. These lesions eliminated the longer latency mode of brainstem projecting CeM neurons, leaving intact the responses of BNST brainstem projecting cells. Compared to the CeM neurons that course through the shorter ventral amygdalofugal pathway, the CeM neurons coursing through the stria terminalis cover a distance 2-3 times as long.

This seems to be a disadvantageous arrangement. However, since the BNST and CeM share major excitatory BL inputs, lengthening the CeM path may allow synchronization of BL driven BNST/CeM inputs to the brainstem. To test this possibility, we compared orthodromic response latencies of CeM and BNST neurons to BL stimuli. The latency difference of the responses of CeM and BNST neurons approximated that seen between the antidromic responses of BNST cells and CeM neurons with long conduction times. These results reveal a previously unsuspected level of temporal coordination between the inputs and outputs of CeM and BNST neurons, supporting the idea of shared functions between these two structures.

3.2) *Methods*

Experiments were performed on rats using an acute *in vivo* setup. Rats were anesthetized with isoflurane. Small openings were made in the skull to allow for recording electrodes to be placed in BNST, CeM, BL, and for stimulating/lesioning electrodes to be positioned in brainstem and stria terminalis. For identification of electrode placements at the end of experiments, the brain was removed, fixed in paraformaldehyde and subsequently sliced and stained. For greater detail regarding above methods, please refer to Chapter II.

3.3) *Results*

A total of 130 CeA and 96 BNST neurons that were spontaneously active and/or responsive to electrical stimuli delivered in the BL or brainstem were

recorded from 48 intact rats in this study. Histological controls (Fig. 3.1B2) revealed that our sample of CeA cells included 102 and 28 neurons recorded in the CeM and CeL, respectively. For BNST cells (Fig. 3.1B1), most were recorded in the anterolateral region (n=83), as defined by Ju and Swanson (1989a, b), with the rest in the posterior (n=13) region.

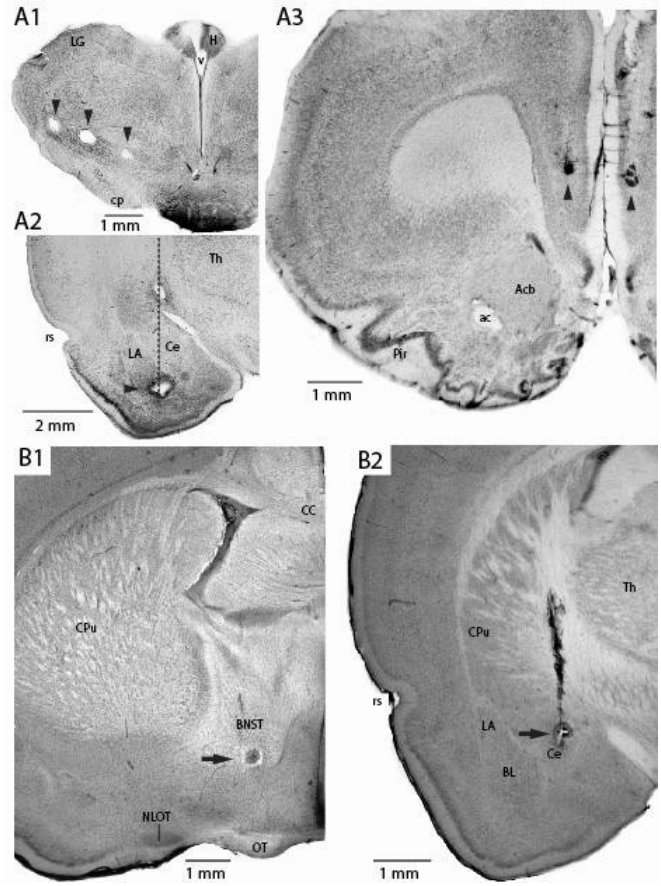

Fig. 3.1 Histological verification of stimulating and recording sites. Coronal sections stained with cresyl violet. (A) Arrowheads point to stimulation sites in the BL nucleus (A1) or dorsal to the substantia nigra (A2). (B) Arrows point to electrolytic lesions in BNST (B1) or CEM (B2), where brainstem-projecting neurons were recorded. Abbreviations: AC, anterior commissure; BL, basolateral nucleus of the amygdala; CC, corpus callosum; CE, central nucleus of the amygdala; cp, cerebral peduncle; CPu, caudate-putamen; H, habenula; LA, lateral nucleus of the amygdala; LG, lateral geniculate nucleus; rs, rhinal sulcus; Th, thalamus; v, ventricle.

Consistent with earlier anatomical findings indicating that CeM has more extensive brainstem projections than CeL (Hopkins and Holstege 1978; Veening

et al., 1984; Petrovich and Swanson 1997), the incidence of brainstem projecting cells, as identified by their antidromic responses to brainstem stimuli, was significantly higher in CeM than CeL (Fisher exact test, $p < 0.001$). Indeed, as many as 76% of CeM cells (or 78 of 102) were antidromically responsive to brainstem stimuli, compared to 32% of CEL cells (or 9 of 28). In the BNST, all antidromically responsive neurons to brainstem stimuli (30% or 29 of 96) were located in the anterolateral region. Thus, below we focus on these anterolateral BNST neurons.

3.3.1) *Latency of brainstem-evoked antidromic responses in CeM and BNST neurons*

Figure 3.2 shows representative examples of CeM (Fig. 3.2 A1-3) and BNST (Fig. 3.2 B1-3) neurons that generated antidromic spikes in response to brainstem stimulation. As shown in the superimpositions of evoked responses (Fig. 3.2 A1, B1), antidromic action potentials could easily be distinguished from synaptically evoked spikes because they had a fixed latency. Moreover, antidromic spikes failed when spontaneous action potentials occurred in the collision interval (Fig. 3.2 A2, B2, Collision). Another property common to CeM and BNST cells was that the transition between the initial segment and somatodendritic components of antidromic spikes was slower than seen in spontaneously occurring action potentials (Fig. 3.2 A1, B1, insets), often giving rise to a clear break between the initial segment and somatodendritic components of the spikes (Fig. 3.2 A1, B1, arrowheads in insets). Consistent

with previous findings in rats (Quirk et al., 2003) and rabbits (Pascoe and Kapp 1985), antidromic response latencies to brainstem stimuli were distributed bimodally in CeM neurons with an early mode at 9.7 ±0.7 ms and late one at 29.4 ± 0.7 ms (Fig. 2A3). Computing the Kolmogorov-Smirnov test for goodness of fit confirmed that the antidromic response latencies of CeA neurons were not normally distributed ($p<0.01$). In contrast, the frequency distribution of brainstem-evoked antidromic response latencies was unimodal in BNST neurons (average of 10.6 ± 0.8 ms; Fig. 3.2B3).

As mentioned in the introduction, previous tract-tracing studies have revealed that CeM axons can reach the brainstem directly, via the ventral amygdalofugal pathway, or through a longer roundabout path, the stria terminalis (Sun et al., 1991). Thus, these findings led us to suspect that the axons of CeM cells with longer conduction times to the brainstem might course through the stria terminalis.

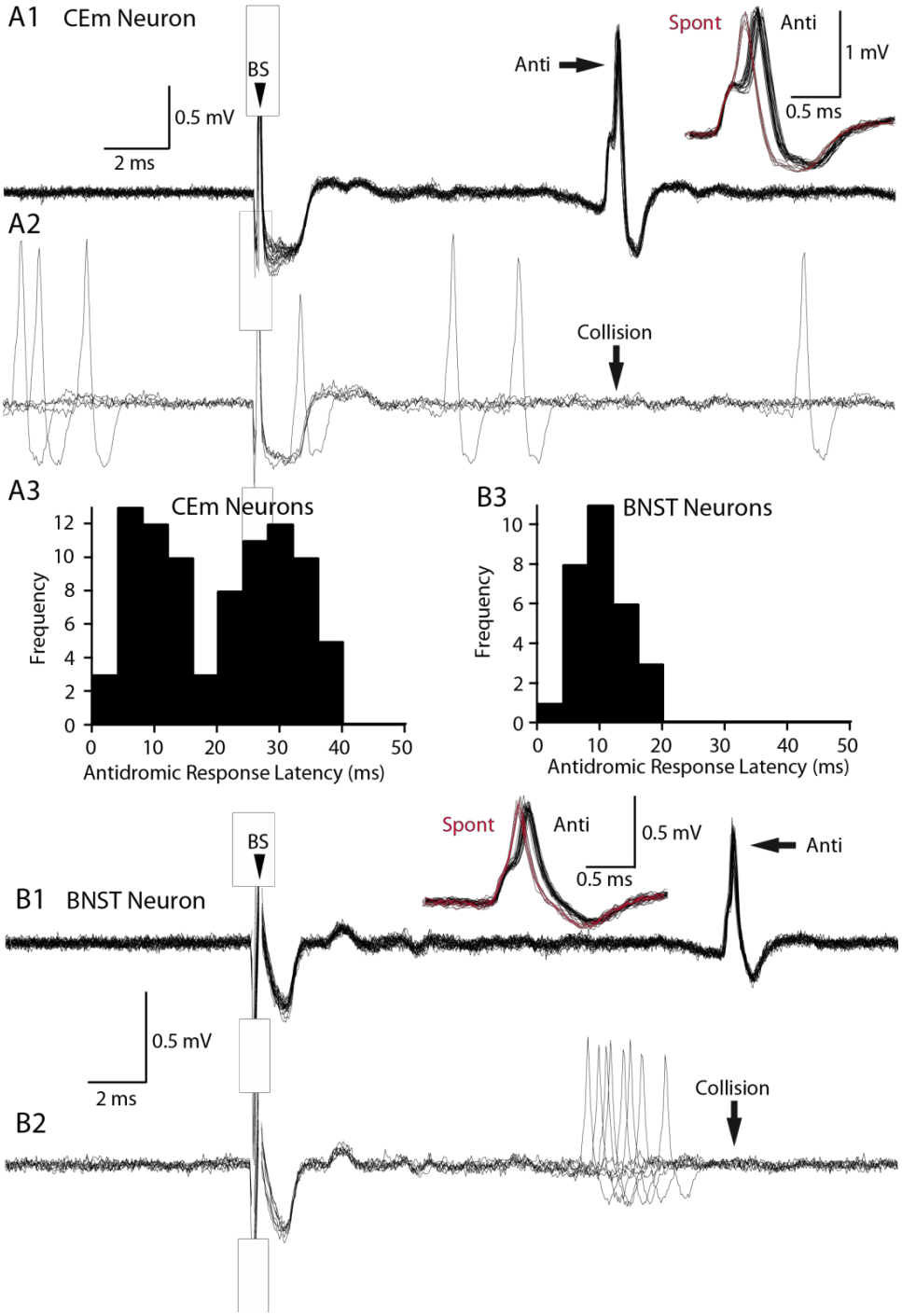

Fig. 3.2 Physiological identification of brainstem-projecting CEM (A) and BNST (B) neurons by antidromic invasion from the brainstem. In A and B, panel 1 shows superimposed antidromic responses to brainstem stimulation, whereas panel 2 shows cases where the antidromic spikes failed because of collision with spontaneous action potentials. The insets in panels 1 show superimpositions of antidromic (black) and spontaneous (red) spikes. Note that the transition between the initial segment and somatodendritic components of the spikes is longer for antidromic action potentials. Panel 3 shows a frequency distribution of antidromic response latencies evoked from the brainstem in samples of 87 CEM and 29 BNST cells.

To test this idea, 26 rats were prepared with electrolytic lesions of the stria terminalis. Post-hoc histological controls revealed that in twelve of these cases the stria was successfully lesioned with minimal damage to adjacent structures (Fig. 3.3A). An additional sample of CeM neurons (n=42) was recorded in these rats and the distribution of brainstem-evoked antidromic response latencies was compared to that seen in intact rats (Fig. 3.3B). For the purpose of statistical comparisons, we used a cut-off of 20 ms to define cells with short vs. long conduction times. In intact rats (Fig. 3.3B, black), our sample of antidromically responsive CeM cells (n=87) was divided equally between cells with short (47%) vs. long (53%) conduction times. By contrast, in rats prepared with lesions of the stria terminalis (Fig. 3.3B, red), our sample of antidromically responsive CeM cells (n=15) was mostly comprised of cells with short conduction times (80% of cells). Using a Fisher exact test, the differing incidence of CeM neurons with short vs. long conduction times to the brainstem in intact vs. stria terminalis lesioned rats was found to be statistically significant ($p = 0.034$)

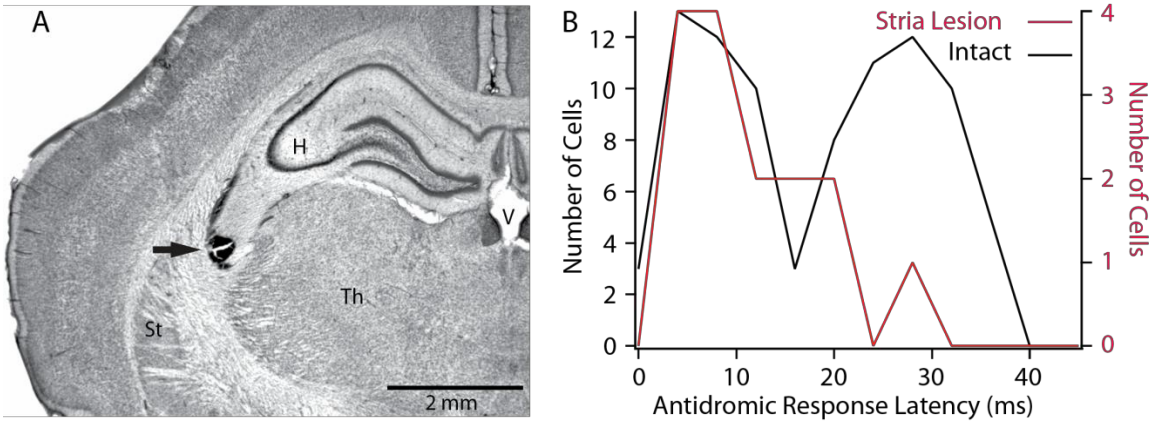

Fig. 3.3 CeM neurons with long conduction times reach the brainstem via the stria terminalis. (A) Coronal section showing electrolytic lesion of stria terminalis (arrow). (B) Frequency distribution of antidromic spike latencies in brainstem-projecting CeM neurons. Black (left y-axis) and red (right y-axis) curves respectively show data obtained in intact rats vs. rats prepared with an electrolytic lesion of the stria terminalis (87 and 15 CEM neurons, respectively). Control data replotted from **Figure 2A3**.

3.3.2) *Latency of BL-evoked orthodromic responses in CeM and BNST neurons*

Compared to the ventral amygdalofugal pathway, the stria terminalis lengthens the path of CeM axons to the brainstem several fold, raising questions as to the significance of this apparently disadvantageous arrangement. Since the BNST and CeM both receive major excitatory inputs from the BL nucleus, we reasoned that lengthening the axonal path of some CeM neurons might allow synchronization of BNST and CeM impulses to the brainstem when they are both activated by BL inputs. To test this idea, we applied electrical stimuli in the BL nucleus and compared orthodromic response latencies in CeM and BNST neurons. Figure 3.4 shows representative examples of BL-evoked orthodromic responses in CeM (Fig. 3.4A1) and BNST (Fig. 3.4B1) neurons (note different time base) and the corresponding peristimulus histograms of neuronal discharges (Fig. 3.4A2, B2). The incidence of such orthodromic responses to BL stimuli was significantly higher among CeM than BNST neurons (CeM, 45% or 46

of 102; BNST, 31% or 26 of 83; Fisher exact test, $p<0.02$). However, the likelihood of observing BL-evoked orthodromic responses was similar for CeM neurons with short vs. long conduction times to the brainstem (Fisher exact test, $p>0.15$). As shown in the representative examples of figure 3.4A1-2, CeM cells generally responded with a pronounced, but brief period of increased firing probability, lasting 3-6 ms. In contrast, the responses of BNST cells were more distributed in time, lasting 10-17 ms (Fig. 3.4B1-2; the origin of this difference is considered in the Discussion).

The contrasting temporal profile of CeM and BNST responses to BL stimuli led us to use two different measures to analyze response latencies: response onset vs. response peak. The latency to response onset was defined as the average of the first two consecutive 1-ms bins of post-stimulus time histograms with counts three times higher than seen in the 10 ms period preceding the BL stimulus. In neurons showing no spontaneous activity during the prestimulus period, the latency to response onset was defined as the average of the first two poststimulus bins with counts. Consistent with the fact that the distance between the stimulation and recording sites is shorter for CeM than BNST neurons, both measures yielded shorter latencies for CeM than BNST neurons. Indeed, using 1.5 times the threshold BL stimulation intensity (usually around 0.3 mA), the average latency to response onset was 7.6 ± 0.4 ms for CeM neurons (n=46; Fig. 3.4A3) compared to 16.5 ± 0.7 ms for BNST neurons (n=26; Fig. 3.4B3). The difference between the latency to response onset of CeM

and BNST neurons was statistically significant (t-test, $p<0.001$). It should be noted that further increases in stimulation intensity did not appreciably reduce the latency to response onset of CeM and BNST neurons. Similarly, as shown in the average peri-stimulus histograms of figure 3.4C, the latency of the response peak was significantly shorter for CeM (8.1 ± 0.4 ms; Fig. 3.4C, thick line) than BNST neurons (23.6 ± 1.1 ms; Fig. 3.4C, thin line; t-test, $p < 0.001$). However, the difference between the two cell groups was much larger with this estimate of response latency. In fact, consistent with our timing hypothesis, the difference in latency to peak was of the same order as that seen between the antidromic responses of BNST cells and CeM neurons with long-conduction times. In closing, it should be mentioned that separate analyses of the latency to peak of BL-evoked responses in BNST neurons with (n=8) vs. without (n=15) physiologically-identified projections to the brainstem yielded qualitatively identical results (respectively, 25.1 ± 3.8 ms and 22.8 ± 2.1ms latencies, t-test, $p>0.05$).

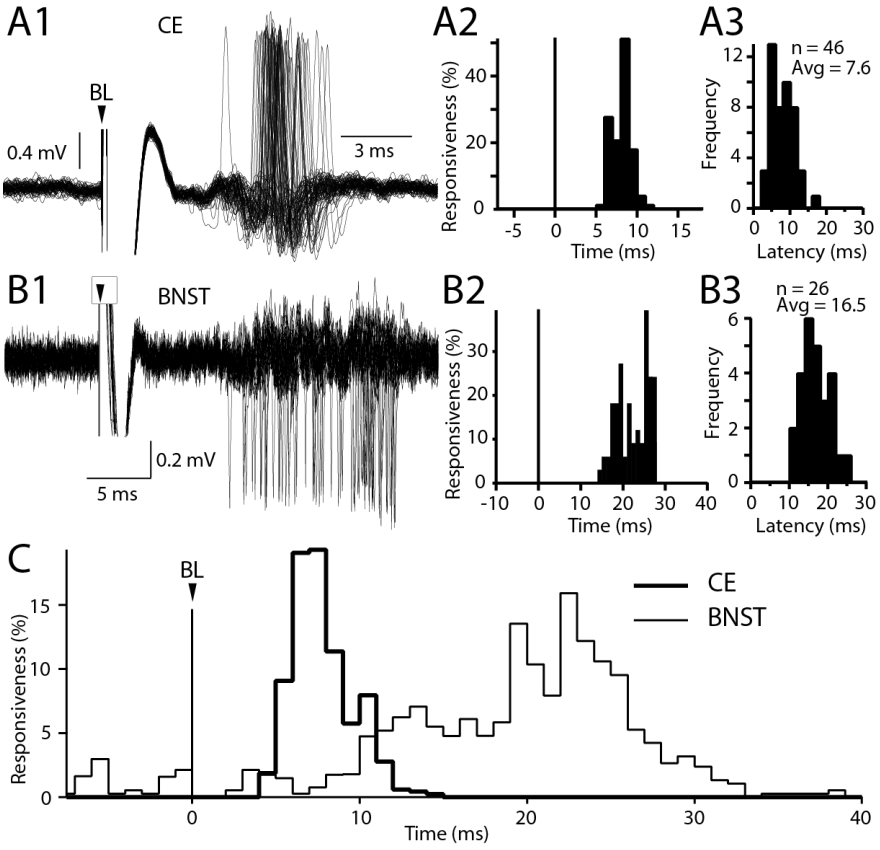

Fig. 3.4 BL stimulation orthodromically actives CEM (A) and BNST (B) neurons. In A and B, panel 1 shows orthodromic responses to BL stimuli, panel 2 shows the corresponding peristimulus histogram of unit discharges, and panel 3 shows the frequency distribution of onset response latencies in samples CEM (A3) and BNST (B3) neurons. (C) Average peri-stimulus histogram of neuronal discharges for CEM (thick line) and BNST neurons (thin line). Prior to averaging, the data of each cell was normalized by dividing the number of spikes in each bin by the number of stimuli. Note that there was a much larger difference between the timing of the response peaks (16 ms difference) than between response onsets (6 ms).

3.4) *Discussion*

The experiments undertaken in the first AIM examined the functional interactions of CeM and BNST neurons with particular emphasis on the relative timing of their brainstem outputs. Our data points to an unexpected level of coordination in the timing of BNST and CeM outputs to brainstem relative to BL inputs. We believe these results support the idea that BL activity can synchronize the outputs of CeM and BNST nuclei in a way that maximizes their postsynaptic

impact on brainstem targets (Fig. 3.5). In support of this hypothesis, we observed a latency of peak BL-evoked responses that was 20 ms longer in BNST cells when compared to CeM cells. This difference approximates the conduction delay introduced by lengthening the path of CeM axons to the brainstem via the stria terminalis. Thus, by lengthening the CeM path to the brainstem, BL driven CeM activity could synchronize with BL driven BNST inputs to the brainstem.

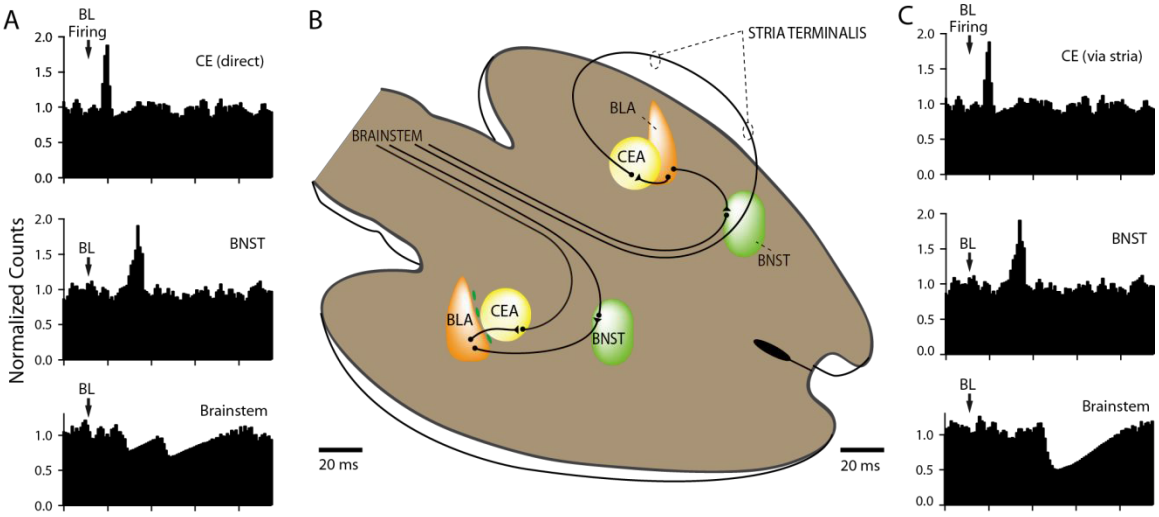

Fig. 3.5 Temporal interactions between BL-evoked activity in CeM and BNST neurons and their hypothesized impact on brainstem cells. (A, C) Artificially generated histograms showing the normalized firing rate (y-axis) of CeM (top), BNST (middle), and brainstem (bottom) neurons after BL discharges (arrows). Panel A shows the impact of CeM cells with direct projections to brainstem (as depicted on the left side of the scheme in B). Panel C shows the impact of CeM cells with axons reaching the brainstem after coursing through the stria terminalis (as depicted on the right side of the scheme in B). The scheme in B shows interconnections between BL, CeM, and BNST. For clarity, CeM cells with direct projections to brainstem are shown on the left whereas those with axons coursing in the stria terminalis are shown on the right. As shown in A, CeM cells with direct projections to the brainstem inhibit brainstem cells at an earlier latency than BNST cells. As shown in C, the delay introduced by having CeM axons reach the brainstem after coursing in the stria terminalis allows temporal summation of the inhibitory effects generated by CeM and BNST cells in brainstem neurons.

CHAPTER IV

AIM #2

SPONTANEOUS ACTIVITY OF BNST NEURONS DURING THE SLEEP-WAKE CYCLE

4.1) *Rationale*

Although much is known about the structure and connectivity of BNSTa, its physiological organization remains poorly understood. A few studies have examined the pharmacological responsiveness (McElligott and Winder 2009; Krawczyk et al., 2011) and electroresponsive properties of BNSTa neurons in brain slices kept in vitro (Egli and Winder, 2003; Hammack et al., 2007; Hazra et al., 2011). The latter reported the presence of three cell types in BNSTa, two of which (regular-spiking, low-threshold bursting) accounted for the majority of the cells (Hammack et al., 2007; Hazra et al., 2011).

Otherwise, the physiological organization of BNSTa remains uncharacterized. Indeed, to the best of our knowledge, with one exception (Terreberry et al., 1995), all extracellular recording studies conducted so far have been performed in deeply anesthetized animals (for instance see Adamec, 1989; Yajeya et al., 1989; Han and Ju, 1990; Veinante and Freund-Mercier, 1998). As a result, we even lack basic information about the spontaneous firing rates and patterns of BNSTa neurons in different states of vigilance. The present study was therefore undertaken to address this gap in our knowledge using multiple simultaneous extracellular recordings in behaving rats.

4.2) *Methods*

Procedures were approved by the Institutional Animal Care and Use Committee of Rutgers University, in compliance with the Guide for the Care and Use of Laboratory Animals (DHHS). Our subjects were male Lewis rats (310-360

g, Charles River Laboratories, New Field, NJ) maintained on a 12 h light/dark cycle. Eight rats were anesthetized using a mixture of isoflurane and O_2, and administered atropine sulfate (0.05 mg/kg, i.m.) to aid breathing. In aseptic conditions, microdrives containing individually moveable bundles of tetrodes were implanted on the heads of the rats. Tetrodes were aimed for BNST-AL and BNST-AM. After a recovery period of 1 week, BNST units were recorded under multiple states of vigilance. Spikes were filtered and clustered using KlustaKwik. At the end of the experiments, animals were deeply anesthetized and small electrolytic lesions were performed to mark recording sites. Brains were extracted and sections were counterstained with cresyl violet. For greater detail regarding above methods, please refer to Chapter II.

4.3) *Results*

4.3.1) *Database*

Histological determination of recording sites (example in Fig. 4.1) revealed that tetrode bundles reached their intended location in 7 of 8 rats. After unit clustering (see Methods), it was determined that samples of 98 BNST-AM and 45 BNST-AL neurons were recorded as the behavioral state of the rats fluctuated spontaneously between waking (W), slow-wave sleep (S) and paradoxical sleep (R).

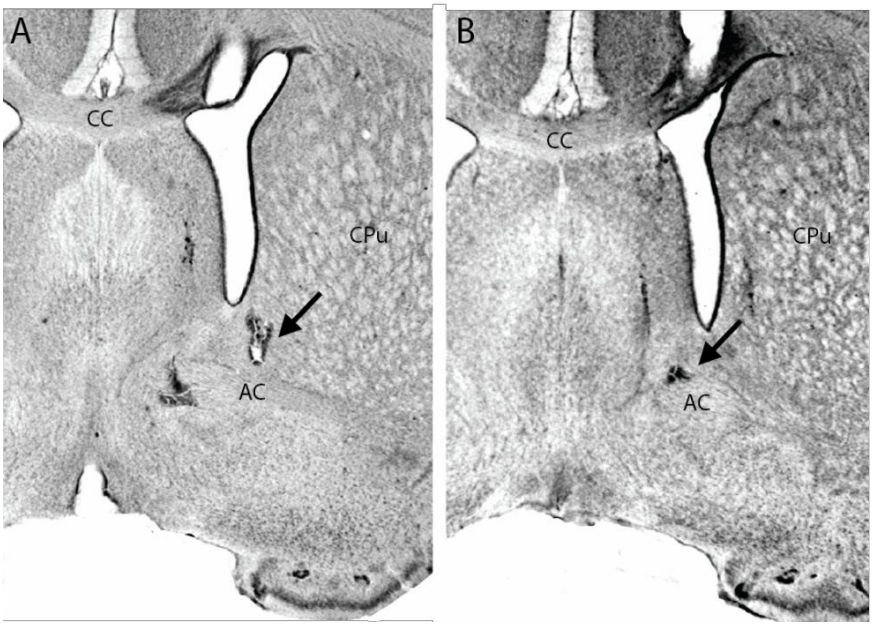

Fig. 4.1 Histological verification of recording sites. Coronal sections stained with cresyl violet. Arrows point to electrolytic lesions marking recording sites in BNST-AL (**A**) and AM (**B**), respectively.

4.3.2) *Identification of behavioral states*

A clear correspondence was seen between the spectral composition of LFPs recorded in BNSTa and behavior. This allowed unambiguous identification of different states of vigilance. During wakefulness, the rats engaged in various types of behaviors (e.g. exploratory locomotion, grooming) and the LFPs were characterized by a relatively low power in the 0-6 Hz range. In addition, theta activity was seen, but only when the animals explored their environment. In contrast, during SWS, the rats were immobile and LFP power in the 0-6 Hz range was markedly higher. When the rats transitioned to REM sleep, the LFP reverted to a waking-like pattern except for the continuous presence of theta activity, in the absence of locomotion. REM and waking could be easily distinguished because rats remained completely immobile in REM sleep, except for occasional muscle twitches.

Figure 4.2 illustrates representative power spectra of LFP activity recorded in BNST-AL (Fig. 4.2A) and AM (Fig. 4.2B) during W (black), S (blue), and R (red). Note that in both BNST-A sectors, the LFP power in the 0-6 Hz range is dramatically higher in S (blue) than W (black) or R (red). In contrast, the power spectra of LFPs recorded in W and REM are similar. However, one consistent difference between these two states was seen in the relationship between theta activity and behavior. In W, theta was only seen when the animals explored their environment. For instance, during the epoch depicted in figure 4.2B, the rat engaged in robust exploratory behavior during waking and a peak was seen in the theta range (8-10 Hz, black trace). In contrast, no such behavior was seen during the epoch shown in figure 4.2A and the power spectrum lacks a peak in the theta range (black trace). Yet, in R sleep, theta activity (Fig. 4.2A1-2, red trace) was seen on background of immobility at both sites. However, theta in R sleep was of a consistently lower frequency than during wakefulness (6-8Hz; insets in Fig. 4.2A, B; paired t-test, $p = 0.01$)

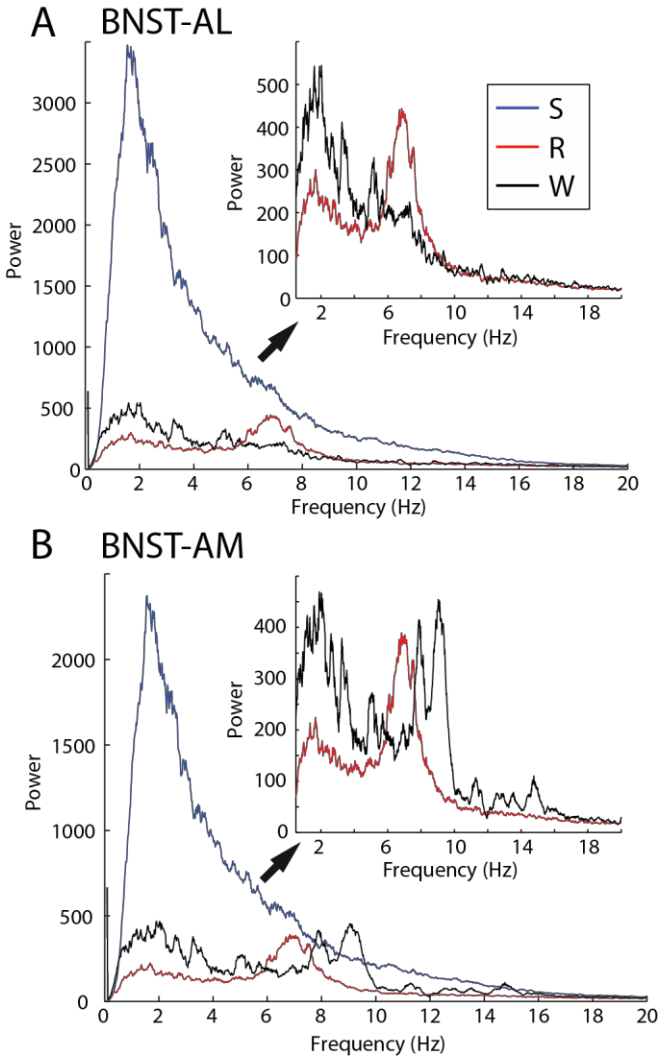

Fig. 4.2 Power spectra of LFPs recorded in BNST-AL (**A**) and AM (**B**) during waking (W, black), slow-wave sleep (S, blue), and REM sleep (R, red). The **insets** in A and B show an expanded version of the waking and REM sleep data to allow a better appreciation of the state dependent shift in theta frequency.

In any given recording session, the rats' state of the vigilance fluctuated between W, S, and R multiple times. This allowed us to assess whether state-related changes in firing rates were reliable (see next section). For instance, figure 4.3A illustrates the spectrogram of a representative session where the rat's behavioral state alternated multiple times between S and R sleep and then transitioned to wakefulness.

Note that in this figure, the spectrogram does not illustrate absolute power values. Instead, power in each frequency band was measured in consecutive 5 sec windows and the fluctuations z-scored. Therefore, the color coding in figure 3A reflects changes in relative power within each frequency band.

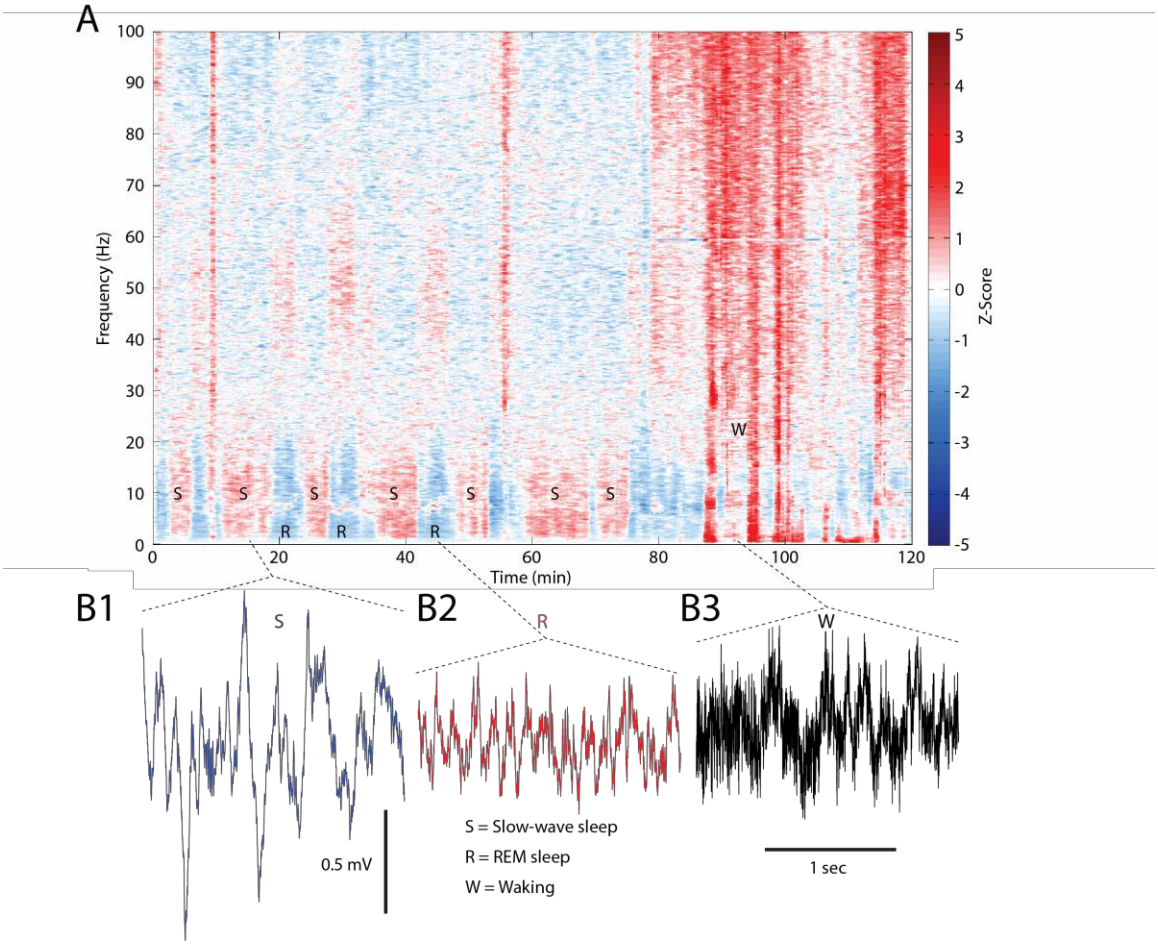

Fig. 4.3 Spectrogram of LFP recorded in BNST-AM during different states of vigilance. (**A**) LFP spectrogram based on a long period of spontaneous activity. (**B1-3**) Examples of LFP activity in S, R, and W, respectively. In **A**, moment-to-moment fluctuations in the power of each frequency was z-scored. Thus, the data shown in the spectrogram is normalized to the average power of each frequency over the entire recording epoch. During the first 80 min, the rat spent most of his time alternating between epochs of S and R. S epochs are characterized by high-amplitude slow waves and reduced power in the gamma range. The opposite profile is seen in R with the exception of a selective increase in power in the low theta range. During the last part of the recording, the rat spent most of the time awake. During this state, power in the 20-100Hz range was increased in a sustained manner.

4.3.3) *State-related changes in firing rates*

The spontaneous firing rates of BNST-AM and -AL neurons ranged widely. In R for instance, when neurons were generally most active, BNST-AM units had discharge rates ranging between 0.03 to 32.4 Hz. A similarly wide range of spontaneous firing rates was observed among BNST-AL cells (0.02 to 24.3 Hz). However at both locations, neurons with low firing rates prevailed. This can be seen in figure 4.4A where frequency distributions of firing rates are provided for the three behavioral states (2 Hz bins). At both recording sites and in all states, neurons with discharge rates <2 Hz accounted for ≥58% of the samples (range 58 to 70%). Because the distribution of firing rates was so skewed, state-dependent changes in firing rates appeared small relative to inter-cell variability (Fig. 4.4B). Nevertheless, as described below, a majority of BNST-AM and AL cells displayed robust state-dependent fluctuations in firing rates.

To determine whether the discharge rates of recorded cells varied depending on the behavioral state, multiple epochs of each state were segmented in 5 sec windows and the firing rate of individual cells was computed for each window. Then, the distribution of firing rates in different states was compared using unpaired t-tests on each cell independently. We decided against using a strict Bonferroni correction of the significance level for multiple comparisons because it would have resulted in absurdly stringent significance levels given the precision of the measurements. For instance, in BNST-AM cells (n=98), with three between-state comparisons (W vs. S, W vs. R, S vs. R), the threshold would have been 0.05/(98 * 3) or 0.00017. Moreover, because sample sizes were different

for BNST-AM (n = 98) and AL (n = 45) neurons, this would have resulted in different significance thresholds for the two cell types. Instead, a between-state difference of firing rate was deemed significant when $p \leq 0.005$ for both cell types.

At both recording sites, a majority (67-86%) of cells exhibited significant changes in firing rates in at least one of the three state comparisons, much greater than expected by chance (0.5%). However, the differences in firing rates between states were not homogenous with different cells showing decreases or increases in firing rate from one state to another. This is shown in figure 4.4C where, for each state comparison, we plot the proportion of cells with a significant change in firing rates in either direction. This reveals a close parallel between BNST-AM (Fig. 4.4C1) and AL (Fig. 4.4C2) neurons. In both cell types, similar proportions of cells showed increases or decreases in firing rates from W to S (Fig. 4.4C, left). In contrast, the distributions were more asymmetric for W vs. R comparisons (middle) and even more so between S and R (right). Chi-square tests comparing this data to random (50-50) distributions revealed that cells with lower firing rates in S than R were significantly more prevalent among BNST-AM and BNST-AL neurons (chi-square tests: AM, $p = 0.000001$; AL, $p = 0.0008$). For the W vs. R comparison, the incidence of cells with higher firing rates in R was significantly higher among BNST-AM neurons, but narrowly missed significance in BNST-AL cells ($p = 0.029$ and 0.053, respectively). For W vs. S comparisons, the proportion of cells with higher firing rates in one state or the other did not differ (AM, $p = 0.26$; AL, $p = 0.65$). Analysis for cells with significant differences in firing rate between states (Fig. 4.4C1) performed using non-parametric measures,

revealed similar results.

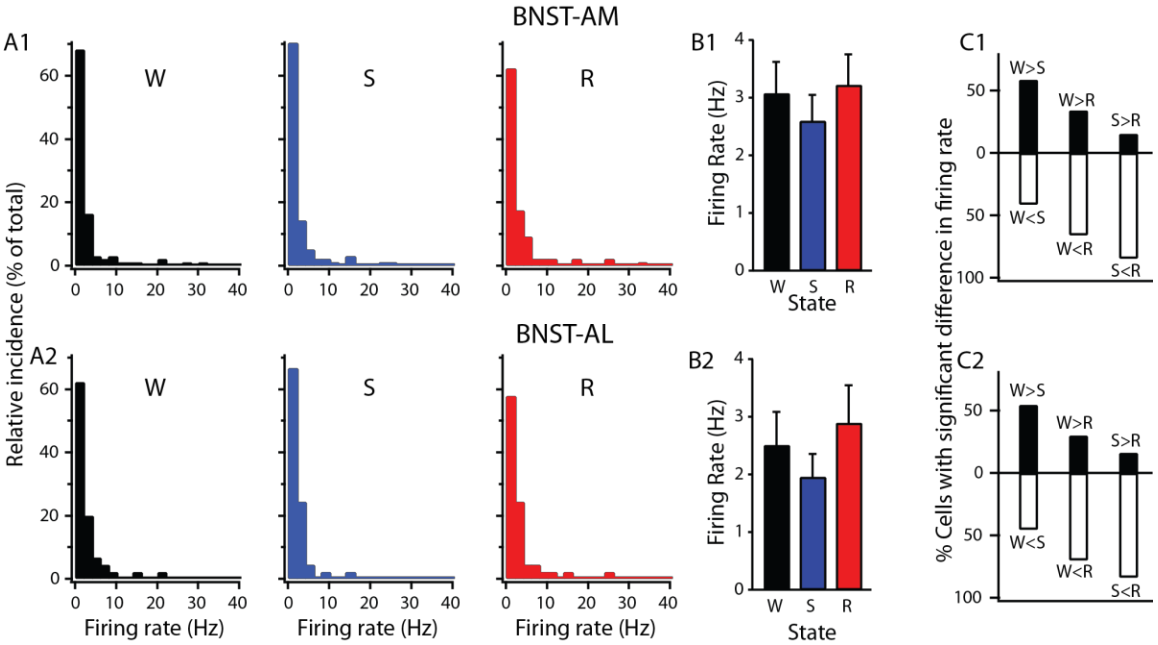

Fig. 4.4 State-dependent fluctuations in the firing rates of BNST-AM (top row) and AL (bottom row) neurons. (**A**) Frequency distributions of firing rates in W (left), S (middle), and R (right). (**B**) Average (±SEM) firing rates (y-axis) in the three states (x-axis). (**C**) Proportion of cells with significant differences in firing rates between W and S (left), W and R (middle) or S and R (right). Cells with firing rate differences in one direction or the other (e.g. W>S or W<S) are plotted separately.

4.4) *Discussion*

Although the connectivity of the BNST is well known, little data is available on its spontaneous activity. To address this gap in our knowledge, I performed recordings of BNST unit and LFP activity during different behavioral states of vigilance. The results I obtained in BNST are reminiscent of the state-dependent changes in activity reported in much of the brain (reviewed in Steriade & Hobson 1976). Indeed, as previously reported in most prosencephalic neurons, the LFPs recorded in BNST showed dramatic alterations when the rats' behavioral state changed. During SWS, LFPs were dominated by large amplitude waves of low frequencies. Upon transition to W or REM sleep, the slow LFP activity was

drastically reduced, giving way to low amplitude irregular waves in a higher frequency range. However, in REM and during active W, prominent theta activity was observed. Theta was of a consistently lower frequency in REM than active W. Most BNSTa neurons fired at very low rates throughout the sleep- waking cycle, with a majority of the cells discharging at less than 2 Hz. Again consistent with earlier reports on neurons in other parts of the prosencephalon (Steriade & Hobson 1976), the firing rates of BNST neurons were generally were lowest in SWS and highest in REM sleep and waking. Overall, these results suggest that BNST is subjected to similar neuromodulatory influences as the rest of the prosencephalon.

CHAPTER V

AIM #3

NEURONAL CORRELATES OF CUED AND CONTEXTUAL FEAR CONDITIONING IN THE BNST

5.1) *Rationale*

The BNST and the CeA are major components of an anatomical entity named the extended amygdala (Alheid and Heimer 1988; de Olmos and Heimer 1999). This notion stems from similarities in the morphology and transmitter content of BNST and CeA neurons (reviewed in McDonald 2003), shared inputs from the basolateral amygdala (Krettek and Price 1978ab; Paré et al. 1995; Savender et al. 1995; Dong et al. 2001a) as well as common projections to brainstem nuclei that generate various aspects of fear/anxiety responses (Hopkins and Holstege 1978; Sofroniew 1983; Veening et al. 1984; Holstege et al. 1985; Dong et al. 2000, 2001b; Dong and Swanson 2003, 2004, 2006a-c).

Despite these anatomical similarities however, the BNST and CeA appear to play different roles. For instance, local drug infusion (Kim et al. 1993; Wilensky et al. 2006), lesion (Hitchcock and Davis 1987, 1991; LeDoux et al. 1988; Campeau and Davis 1995; Jimenez and Maren 2009), optogenetic (Ciocchi et al. 2010) and unit recording studies (Duvarci et al. 2011) suggest that CeA is required for the rapid expression of conditioned fear responses to discrete sensory cues (however see Koo et al. 2004; Pitts et al. 2009), functions that are left intact by BNST lesions (Walker and Davis 1997; Gewirtz et al. 1998; Sullivan et al. 2004). Instead, BNST lesions interfere with the development of longer “anxiety-like” states in response to more diffuse environmental contingencies, responses that often persist after the threat has vanished (reviewed in Walker et al. 2003; Sullivan et al. 2004; Duvarci et al. 2009). In particular, BNST lesions

were reported to disrupt corticosterone and freezing responses to contextual stimuli that were previously associated with aversive outcomes (Sullivan et al. 2004). Importantly, dissociation between CeA and BNST functions is not only seen in aversive learning paradigms but also in response to some unconditioned stimuli (Fendt 2003).

Given their common inputs from the basolateral amygdala and overlapping projections to fear effector neurons, the basis for the functional dissociation between BNST and CeA is unclear. Thus, the question of the specific contribution each nucleus makes to conditioned fear remains. To shed light on this question, we recorded anterior BNST neurons in freely moving rats subjected to an auditory fear conditioning paradigm.

5.2) *Methods*

Procedures were approved by the Institutional Animal Care and Use Committee of Rutgers University, in compliance with the Guide for the Care and Use of Laboratory Animals (DHHS). Our subjects were male Lewis rats (310-360 g, Charles River Laboratories, New Field, NJ) maintained on a 12 h light/dark cycle. Eight rats were anesthetized using a mixture of isoflurane and O_2, and administered atropine sulfate (0.05 mg/kg, i.m.) to aid breathing. In aseptic conditions, microdrives containing individually moveable bundles of tetrodes were implanted on the heads of the rats. Tetrodes were aimed for BNST-AL and BNST-AM. After a recovery period of 1 week, rats were exposed to a differential fear conditioning paradigm. BNST units were recorded for all phases of the behavioral fear conditioning paradigm. Spikes were filtered and clustered using

KlustaKwik. At the end of the experiments, animals were deeply anesthetized and small electrolytic lesions were performed to mark recording sites. Brains were extracted and sections were counterstained with cresyl violet. For greater detail regarding above methods, please refer to Chapter II.

5.2.1) *Statistical analyses*

To assess whether CS-evoked responses were significant, we first computed the firing rate of each unit in 5 sec bins, from 20 s before to 120 s after the onset of the CS^+ and CS^-. Separate averages were obtained for the habituation phase, the first two and last three CS^+ and CS^- of training, as well as the first and last five CS^+ and CS^- of the two recall tests. The data of each average was then z-scored to firing rate variations seen in the pre-CS period. A CS-evoked change in firing rate was deemed significant, when the six 5-s bins of the CS^+ or CS^- differed from the baseline period by ±1.96 z or more. This corresponds to a significance threshold of $p \leq 0.05$. To assess whether the proportion of responsive cells changed significantly depending on the phase of the behavioral protocol, we used a chi-square test that analyze whether there was a dependence between response type (response, no response) and behavioral phase (habituation, CS^+ 1-2 or 3-5 of training, first 5 or last 5 CS^+ of the two recall tests.

5.3) *Results*

As shown in figure 5.1B1, all our recordings were obtained dorsal to the anterior commissure, in the anterior third of BNST. Previously, this BNST region was divided in multiple subnuclei based on cytoarchitectural and immunohistochemical criteria (Ju and Swanson 1989ab). However, due to the difficulty of unambiguously identifying these subnuclei in sections stained with cresyl violet, we simply divided our recording sites in two groups, based on their position relative to the intra-BNST component of the stria terminalis. Indeed, this fiber bundle separates the anterior BNST in two large sectors: BNST-AM and BNST-AL. The correspondence between these two regions and the subnuclei identified by Swanson and colleagues is as follows: BNST-AL corresponds to Swanson's oval, juxtacapsular, and anterolateral subnuclei. BNST-AM corresponds to Swanson's anterodorsal subnucleus. Note that in more recent publications (Dong and Swanson 2006a) Swanson also terms the latter region BNST-AM.

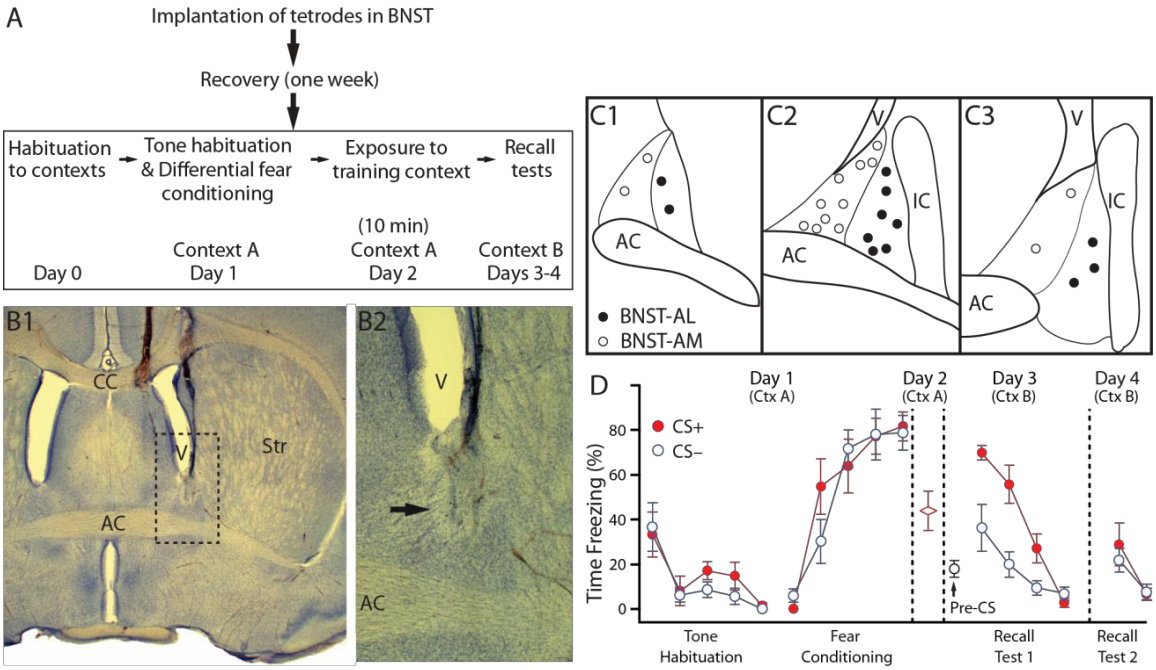

Figure 5.1. Experimental paradigm, location of recording sites, and behavioral results. (**A**) Experimental paradigm. After implantation of tetrodes in BNST and recovery from surgery, rats were subjected to a differential auditory fear conditioning paradigm. On day 0, rats were habituated to the training contexts A and B. On day 1, in context A, they were first habituated to the CS+ and CS- and then subjected to fear conditioning session where the two CSs were presented an equal number of time in random order with only the CS+ co-terminating with a footshock. On day 2, they were exposed to the training context A with no tone presentations to assess contextual fear. On days 3-4, two recall tests were conducted in context B. (**B**) Sample histological verification of recording site. (**B1**) Photomicrograph showing a coronal section at the level of BNSTa. Arrow points to small electrolytic lesion performed at the conclusion of the experiment to mark a recording site. The area enclosed in the dashed rectangle is expanded in (**B2)**. Abbreviations: AC, anterior commissure; CC, corpus callosum; Str, striatum, V, ventricle. (**C**) Location of well positioned tetrodes. Three antero-posterior levels arranged from the most rostral (**C1**) to the most caudal (**C3**). Filled and empty circles represent tetrode placements in BNST-AL and AM, respectively. (**D**) Percent time (average ± sem) the rats (n-8) spent freezing during the CS^{+} (red circles), CS^{-} (blue circles) or during exposure to the training context (red diamond) in various phases of the behavioral protocol (x-axis). For Day 1, we plot freezing to individual CSs. For Days 3-4, blocks of 5 CSs were used to compute the averages. Empty black circle indicates pre-CS freezing during recall test 1. Note that 5 minutes elapsed between placement of the rats in context B and presentation of the first CS. Pre-CS freezing was measured the last four minutes of this period.

5.3.1) *Database*

Histological verification of recording sites (Fig. 5.1B-C) revealed that tetrodes reached their intended targets (BNST-AL and/or AM) in seven of the eight rats. Units recorded with misplaced tetrodes were excluded from the

analyses. Overall, samples of 47-56 BNST-AL and 65-105 BNST-AM units were recorded on each day of the conditioning protocol. The locations of well-positioned tetrodes are shown in figure 1C. Electrodes were not moved during the behavioral protocol unless units were lost overnight across all tetrodes within a bundle. In such rare cases, the tetrode bundle was lowered 60 μm. Although the electrodes were generally not moved, spike shapes varied from day to day in a proportion of units. Therefore, below it is assumed that different cells were recorded on each day.

5.3.2) *Impact of differential fear conditioning*

After electrode implantation and recovery from surgery, rats were trained on cued (auditory) fear conditioning while recording BNST activity. As summarized in figure 5.1A, the behavioral protocol included habituation to the training contexts (Fig. 5.1A, Day 0) followed the next day by habituation to the auditory CS^+ and CS^-, and then differential fear conditioning in Context A (Fig. 5.1A, Day 1). Twenty-four hours later, contextual fear memory was assessed in context A for 10 minutes (no CS; Fig. 5.1A, Day 2). Finally, two recall tests of cued fear memory were performed on consecutive days in Context B (Fig. 5.1A, Days 3 and 4).

Figure 5.1D illustrates the percent time rats spent freezing during the various phases of the behavioral protocol. Red and blue circles represent freezing to the CS^+ and CS^-, respectively. The red diamond represents contextual freezing in Context A. Relative to the last CS^+ and CS^- of habituation,

fear conditioning caused a significant increase in freezing levels to the CS^+ (CS^+ 5, 81.9 ± 6.5%) and CS^- (CS^- 5, 78.9 ± 7.8%, paired t-tests, $p < 0.001$). The next day, in the absence of auditory stimuli, the rats exhibited robust freezing to the training context (A, 43.9 ± 8.8%, red diamond). On day 3, rats showed little freezing prior to presentation of the auditory stimuli (pre-CS freezing: 17.9 ± 3.8%; black circle) in Context B. However, the first few CS^+ elicited large increases in freezing (CS^+ 1-5: 69.9 ± 3.2%) that gradually diminished with additional CS^+ presentations (CS^+ 16-20: 2.8 ± 2.2%, paired t-test, $p<0.001$). Although discrimination between to CS^+ and CS^- was imperfect, freezing to the CS^- (CS^- 1-5, 36.3 ± 10.5%) was significantly lower than to the CS^+ (paired t-test, $p = 0.002$). On Day 4, the first few CS^+ presentations again elicited freezing (CS^+ 1-5: 28.8 ± 9.5%) that extinguished with additional presentations of the CS^+ (CS^+ 6-10: 6.6 ± 2.7%).

Overall, these results suggest that the differential auditory fear conditioning paradigm used in this study led to the formation of a fear memory to the training context and CS^+. Although discrimination between the CS^+ and CS^- was imperfect, fear responses to the CS^+ were clearly stronger than to the CS^- during the first recall test.

5.3.3) *Cellular correlates of cued fear memory in BNST-AL and AM*

To analyze training-induced changes in auditory responsiveness, we first computed the firing rate of each unit in 5 sec bins, from 20 s before to 120 s after the onset of the CS^+ and CS^-. We obtained separate averages for the habituation

phase, the first two and last three CS^+ and CS^- of training, as well as the first and last five CS^+ and CS^- of the two recall tests. For each average we then z-scored the data to firing rate variations seen in the pre-CS period. Next, to determine whether a CS-evoked change in firing rate was significant, we separately averaged the z-scores of each cell during the six 5-s bins of the CS^+ or CS^- and assessed whether it differed from the baseline period by ±1.96 z or more (yielding a significance threshold of $p \leq 0.05$). The results of these analyses are shown in figures 5.2-5.6, including group analyses and individual examples of significantly responsive cells.

Figure 5.2 illustrates the proportion of cells responsive to the CS^+ (Fig. 5.2A1) or CS^- (Fig. 5.2A2) in the different phases of the behavioral protocol, combining the results obtained in BNST-AL and AM. The proportion of responsive cells changed depending on the phase of the behavioral protocol. To determine if these changes were statistically significant, we used a chi-square test. This analysis revealed a significant dependence ($p < 0.0001$) between response type to the CS^+ (response, no response) and behavioral phase (habituation, CS^+ 1-2 or 3-5 of training, first 5 or last 5 CS^+ of the two recall tests).

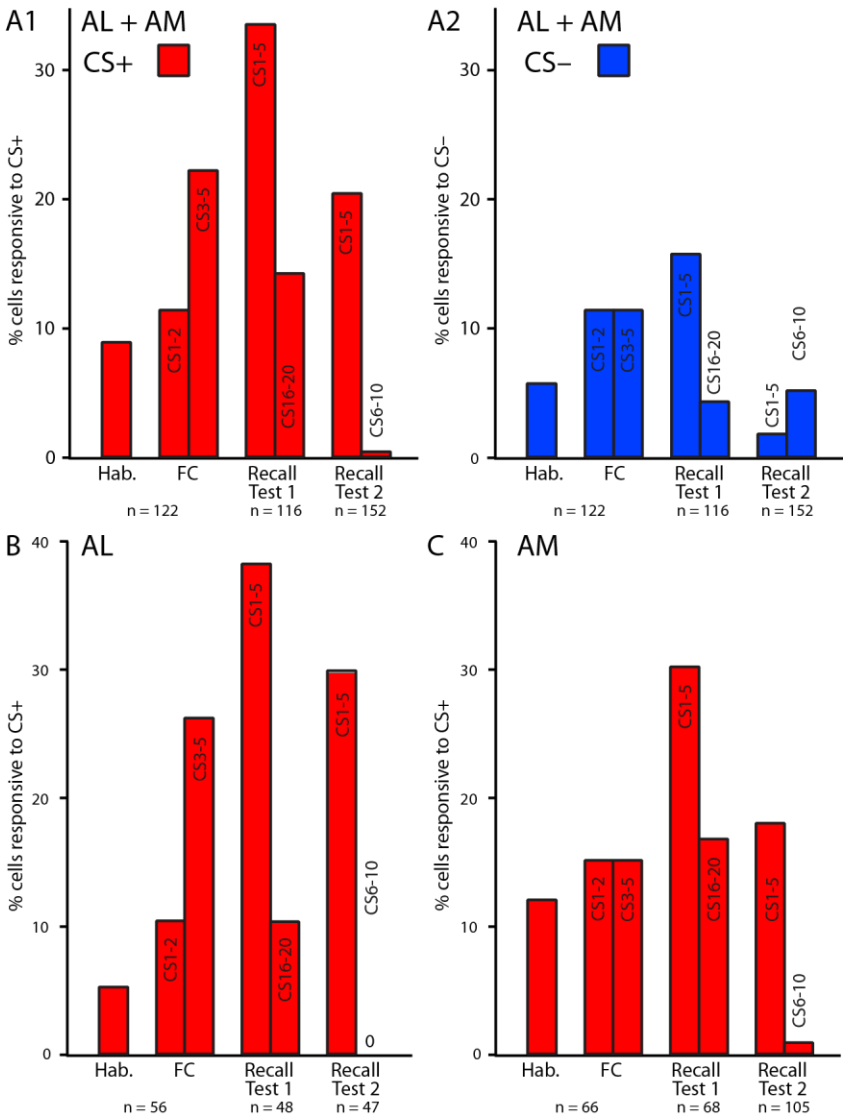

Figure 5.2. Differential fear conditioning alters the responses of BNST neurons in a CS-specific manner. Proportion of BNST cells (AL and AM combined) with significant responses (increased or decreased) to the CS^+ (**A1**) or CS^- (**A2**) during the various phases of the behavioral protocol (x-axis). In **B** and **C**, the same data as in **A** is plotted but considering BNST-AL (**B**) and AM (**C**) neurons separately. In **A-C**, the number of recorded cells is indicated at the bottom of the graphs.

Paralleling our behavioral observations, the proportion of cells responsive to the CS^+ (Fig. 5.2A1) and CS^- (Fig. 5.2A2) was low during habituation, and it increased significantly as a result of fear conditioning (χ^2 test, habituation vs. CS^+ 3-5 of training, $p = 0.003$). The proportion of responsive cells was significantly higher for the CS^+ than the CS^- at the end of training (χ^2 test, $p = 0.015$). Without

exception, all cells with significant responses to the CS^- were also responsive to the CS^+ and the two CSs elicited responses of the same polarity (see below). Interestingly, the proportion of CS^+-responsive cells increased further from the end of fear conditioning to the first recall test two days later (χ^2 test, p = 0.03) and was significantly higher than that to the CS^- (χ^2 test, p = 0.001). Additional presentation of the CS^+ during the two recall tests caused a progressive reduction in the proportion of CS^+-responsive cells such that it became statistically indistinguishable from that seen during habituation by the end of the second recall test.

A similar pattern of results was obtained when we separately considered BNST-AL (Fig. 5.2B) and BNST-AM (Fig. 5.2C) units, with one interesting exception. Indeed, the timing of the increase in CS^+-responsiveness differed in the two cell types. In BNST-AL units, the increase was apparent by the end of training (CS^+ 1-2 vs. CS^+ 3-5 of fear conditioning, χ^2 test, p = 0.003) and it became even more pronounced during the recall test (CS^+ 1-2 of training vs. CS^+ 1-5 of recall test 1, p = 0.0003). In contrast, in BNST-AM cells, no change occurred from the beginning to the end of training. The increase in the proportion of responsive cells only became apparent two days later, during the first recall test (CS^+ 1-2 of training vs. CS^+ 1-5 of recall test 1, χ^2 test p = 0.015).

In the analyses presented so far, we considered all cells with significant responses to the CS^+ together, whether their responses consisted of an increase or a decrease in firing rate. We now consider the polarity of their responses. As shown in figure 5.3, the relative incidence of cells with inhibitory (blue; “Off-cells”)

vs. excitatory (red, “On-cells”) responses to the CS^+ differed between BNST-AL and AM. In BSNT-AL (Fig. 5.3A), fear conditioning caused a large increase in the proportion of Off-cells (CS^+ 1-2 vs. 3-5 of training, χ^2 test, $p = 0.0022$) with little change in the incidence of On-cells. Two days later, during the first 5 CS^+ of the recall test, the incidence of Off-cells remained similarly high whereas the proportion of On-cells augmented. However, the latter change did not reach significance. With additional presentations of the CS^+, roughly equal but decreasing proportions of cells showed inhibitory and excitatory responses.

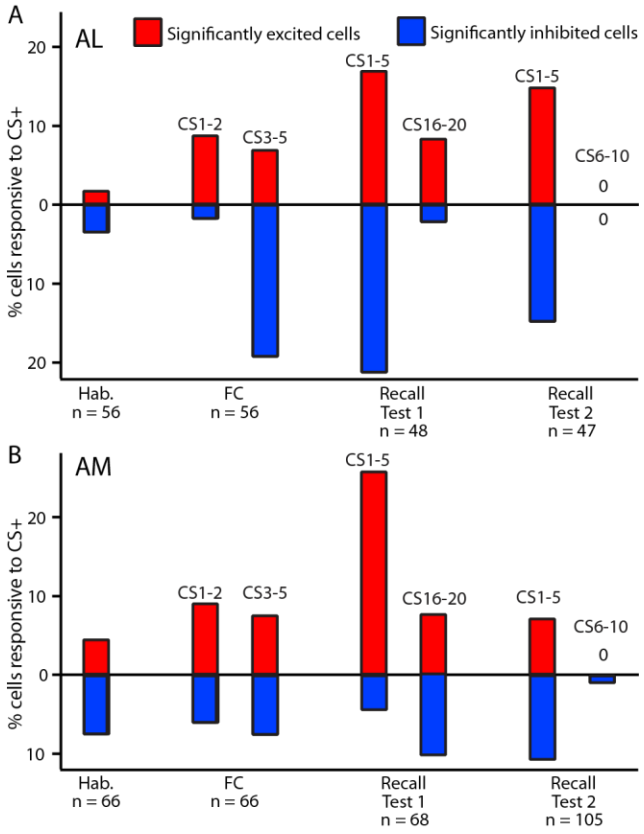

Figure 5.3. Opposite polarity of changes in CS responsiveness in BNST-AL vs. AM neurons. Proportion of BNST-AL (**A**) and AM (**B**) cells with significant excitatory (red) or inhibitory (blue) responses to the CS^+ during the various phases of the behavioral protocol (x-axis). The number of recorded cells is indicated at the bottom of the graphs.

Figure 5.4A illustrates a representative example of a BNST-AL neuron with

inhibitory responses to the CS^+ during the first recall test. In the top panel, each of the twenty lines shows the activity of the cell from the first (top) to the last (bottom) CS^+ (gray shading) of recall test 1. The bottom panel shows the average firing rate of the same cell during the first (red) and last (black) five CS^+ of the first recall test. The first five CS^+ elicited a sustained decrease in firing rate, essentially silencing the cell for the entire duration of the CS^+. Across all BNST-AL cells with inhibitory responses to the CS^+, the firing rate during the first five CS^+ of recall test 1 decreased to 27.3 ± 10.8% of baseline. Additional presentations of the CS^+ caused a reduction of the CS^+-evoked inhibition (CS^+16-20, to 48.5 ± 12.1% of baseline; paired t-test, $p = 0.00011$).

In contrast with the results obtained in BNST-AL, the proportion of BNST-AM units with inhibitory or excitatory responses to the CS^+ did not change on the training day (compare CS^+ 1-2, vs. 3-5 of training in Fig. 5.3B). Two days later, during the first 5 CS^+ of the recall test, a large and significant increase in the incidence of On-cells was observed (CS^+ 3-5 of training vs. CS^+ 1-5 of recall test 1, χ^2 test, $p = 0.0021$) with little change in the proportion of Off-cells. Additional presentations of the CS^+ reduced the incidence of On-cells.

Figure 5.4B illustrates a representative example of a BNST-AM neuron with excitatory responses to the CS^+ during the first day of recall testing. Typical for these cells, the increase in firing rate elicited by the CS^+ peaked during the first 5 sec of the CS and then decreased later on. Also typical for these cells, additional presentations of the CS^+ during the recall test, caused a reduction of their responses (from 137.6 ± 6.5% of baseline to 105.7 ± 4.2% during the first 5

and last 5 CS^+, respectively; paired t-test, p = 0.00055).

Although the examples of BNST-AL and AM cells shown in figure 5.4 exhibited different baseline firing rates, this was not a general trend in our samples. In both regions, spontaneous firing rates ranged widely, with cells firing between 1 to 4 Hz being most common. During the pre-CS period of the first recall test, the spontaneous firing rates of BNST-AL (2.22 ± 0.54 Hz) and BNST-AM (3.14 ± 0.82 Hz) neurons did not differ significantly (t-test, p=0.43).

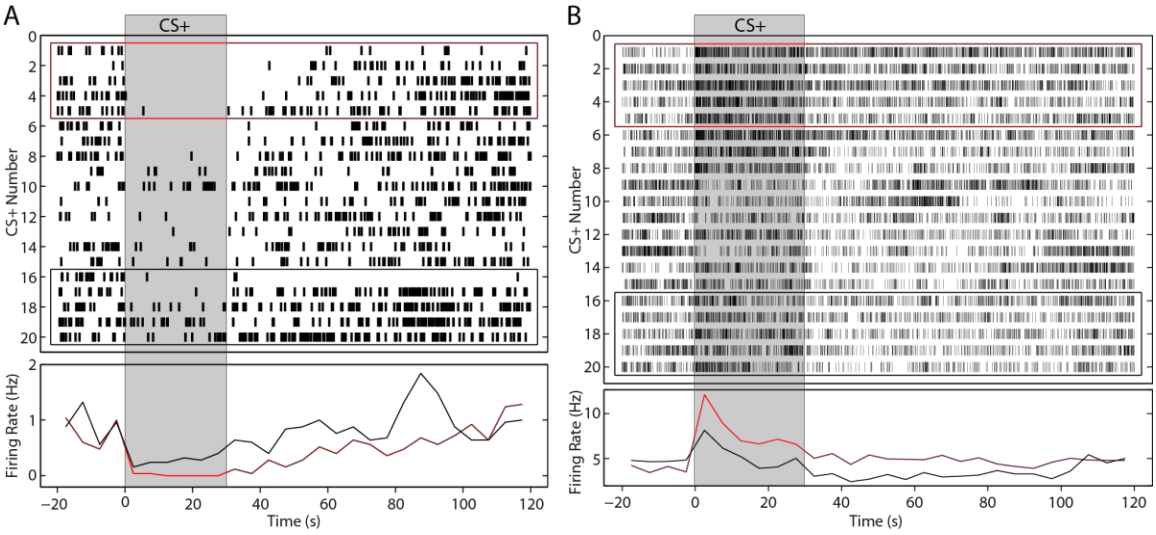

Figure 5.4. Examples of BNST neurons with inhibitory and excitatory CS^+ responses during first day of recall testing. (**A**) BNST-AL cell with inhibitory response to the CS^+. (**B**) BNST-AM neurons with excitatory responses to the CS^+. In the **top panel** of **A** and **B**, each of the twenty horizontal lines shows the activity of the cell from the first (top) to the last (bottom) CS^+ (gray shading) of recall test 1. Each vertical tick represents one action potential. The bottom panel shows the average firing rate of the same cells during the first (red) and last (black) five CS^+.

In the chi-square analyses presented in figures 5.2-5.3, we reported on the incidence of cells with significant responses to the CSs. A limitation of this approach when comparing two cell groups is that it ignores the magnitude of the changes in responsiveness. To address this potential confound, we next compared the average responses of BNST-AL (Fig. 5.5) and AM (Fig. 5.6) cells

from habituation to the end of training (left) and during the recall test (right). Separate averages are provided (from top to bottom) for all cells combined, On-cells, and Off-cells. Comparing the average behavior of BNST-AL and AM neurons during the recall test (Figs. 5.5B and 5.6B, respectively) reveals striking differences that are consistent with the incidence analyses presented in figure 5.3. Due to response heterogeneity among BNST-AL neurons (Fig. 5.5B2, C2), no significant change in CS responsiveness is seen in the grand average of all BNST-AL neurons from the beginning (red) to the end (black) of the first recall test. This contrasts with the grand average of all BNST-AM neurons (Fig. 5.6B1) where, due to the prevalence of On-cells (Fig. 5.6B2), a robust increase in activity is apparent at the onset of the recall test (Fig. 5.6B1, red).

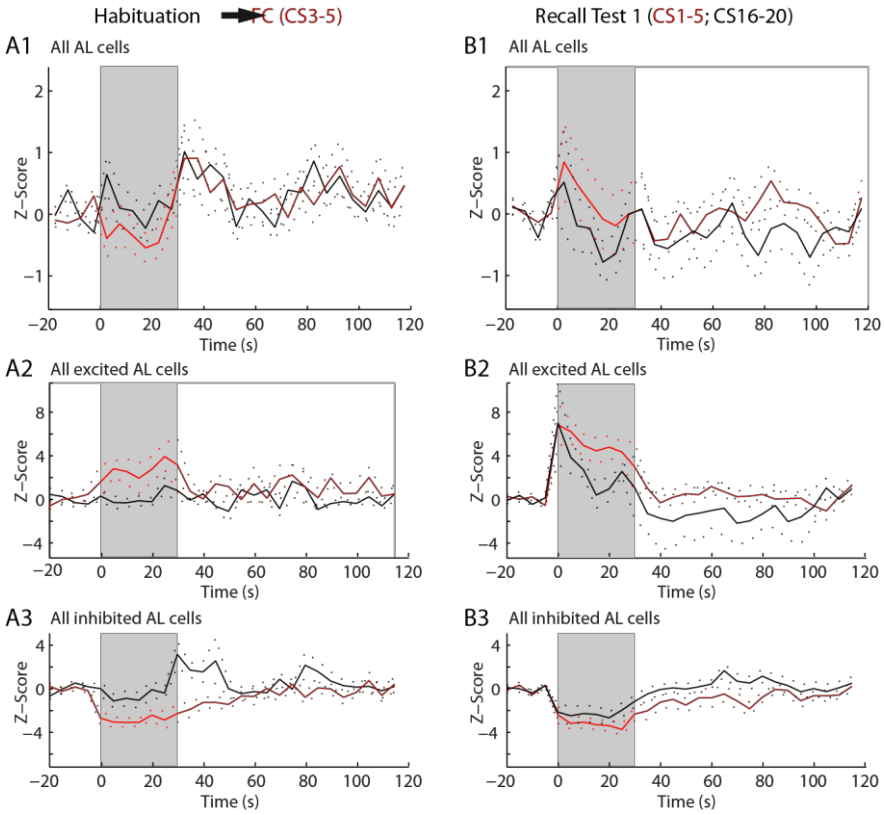

Figure 5.5. Grand average of the responses of BNST-AL neurons to the CS^+ (gray shading) (**A**) during habituation (black) and at the end of training (red) as well as (**B**) during the recall test (red and black: first and last 5 CS^+, respectively). In **A1** and **B1**, all available BNST-AL cells were included in the averages, whereas the averages shown in panels 2 and 3 were restricted to cells with significant excitatory or inhibitory responses, respectively. Dotted lines represent the SEM.

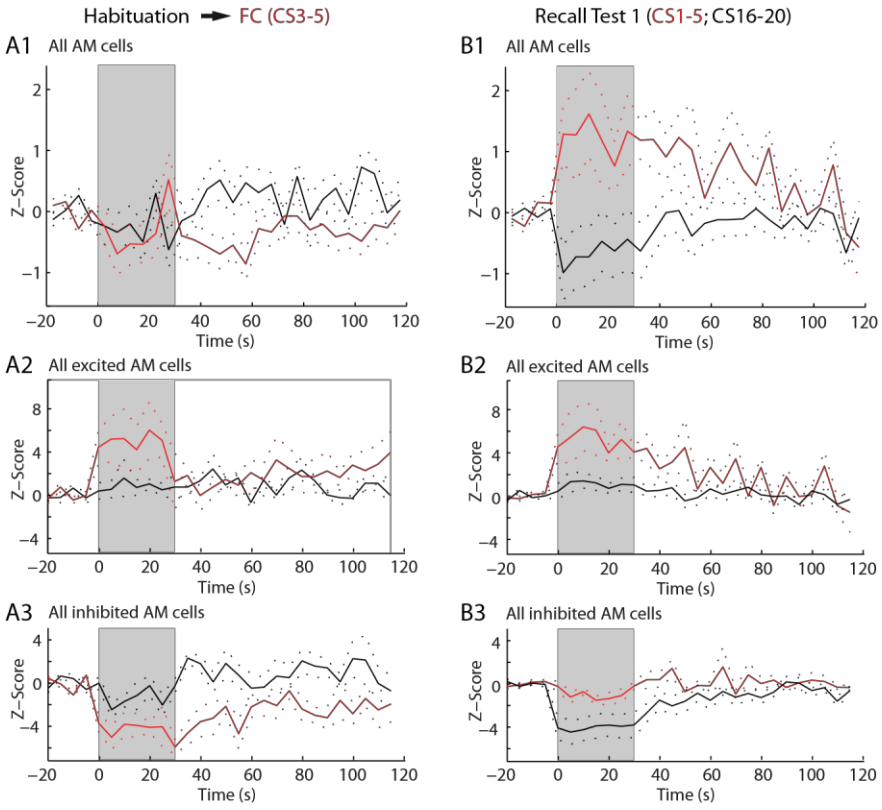

Figure 5.6. Grand average of the responses of BNST-AM neurons to the CS^+ (gray shading) (**A**) during habituation (black) and at the end of training (red) as well as (**B**) during the recall test (red and black: first and last 5 CS^+, respectively). In **A1** and **B1**, all available BNST-AM cells were included in the averages, whereas the averages shown in panels 2 and 3 were restricted to cells with significant excitatory or inhibitory responses, respectively. Dotted lines represent the SEM.

5.3.4) *Cellular correlates of contextual fear memory in BNST-AL and AM*

Because prior behavioral studies have revealed that BNST lesions reduce contextual fear (Sullivan et al. 2004; Duvarci et al. 2009), we next studied the activity of BNST-AL (n = 38) and AM (n = 69) neurons during the 10-min exposure to the training context on day 2, when the rats exhibited high levels of contextual freezing (Fig. 5.1D, red diamond). We observed that most BNST-AM cells fired at a higher rate during freezing than movement whereas BNST-AL cells tended to show the opposite behavior. Representative examples of BNST-AM and AL neurons with respectively higher and lower activity during behavioral

freezing than movement are provided in figure 5.7A and B, respectively.

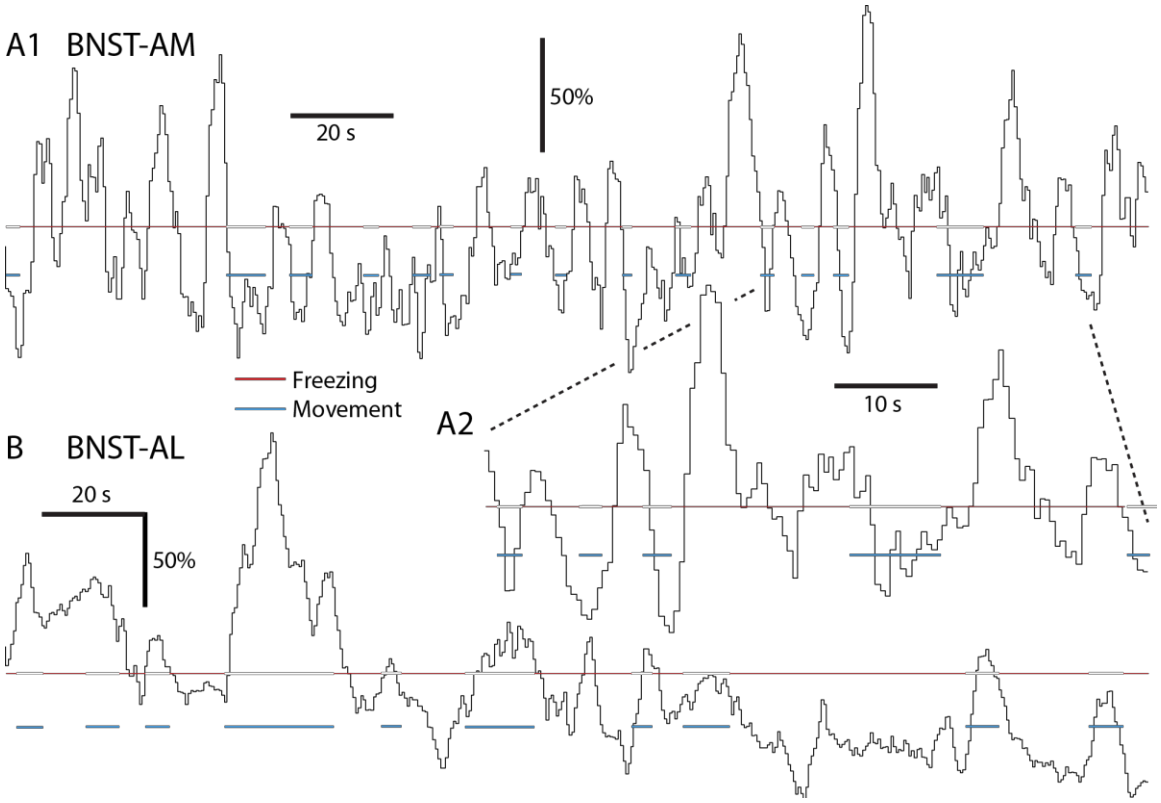

Figure 5.7. Differential activity of BNST-AM and AL neurons during movement vs. contextual freezing. Black traces depict normalized fluctuations in firing rate during periods of freezing (red lines) and movement (blue lines). (**A**) Fluctuations in the firing rate of five simultaneously recorded BNST-AM cells, expressed as percent of average. A portion of **A1** (dashed lines) is shown with an expanded time base in **A2**. (**B**) Fluctuations in the firing rate of three simultaneously recorded BNST-AL cells, expressed as percent of average. In **A** and **B**, prior to averaging, the firing rates of individual cells was normalized to the average of the entire period so as to give and equal weight to the data obtained in each cell. Note that to optimize the temporal resolution of the behavioral measurements, the exact onset and offset times of visually identified periods of freezing and movement were determined using frame-by-frame analysis of the video recordings. Data depicted in A and B was obtained in different rats.

To address this quantitatively, we compared the firing rate of each cell during multiple epochs of freezing vs. movement. The spike trains were first smoothed with a Gaussian kernel with a standard deviation of 0.25 s. The resulting rate estimate was then sampled at 0.5 s intervals and periods of freezing and movement were compared using an unpaired t-test, in each cell independently (Fig. 5.8A). As shown in figure 5.8B, a higher proportion of BNST-

AM (47.8% or 33 of 69) than BNST-AL cells (28% or 11 of 38) fired at significantly different rates in epochs of high vs. low fear (Fisher exact, p = 0.027). Not only was the proportion of neurons with differential activity dissimilar in the two BNST regions, so was the prevalent polarity of the difference (Fig. 5.8B). Indeed, paralleling the pattern of results seen with responses to the CS^+, the majority of significant BNST-AM cells (66.6% or 22 of 33) fired at higher rates during freezing than movement whereas most significant BNST-AL cells did the opposite (63.6% or 7 of 11; Fisher exact, p = 0.062).

These results were confirmed using a different statistical approach, namely correlating motor activity (freezing = 1; movement = 0) and firing rates across multiple 0.5 s windows and testing whether the correlation is significant. Panels C1 and C2 of figure 5.8 show examples BNST-AM and AL neurons with significant negative and positive correlations to movement, respectively. This statistical approach yielded nearly identical results to the above.

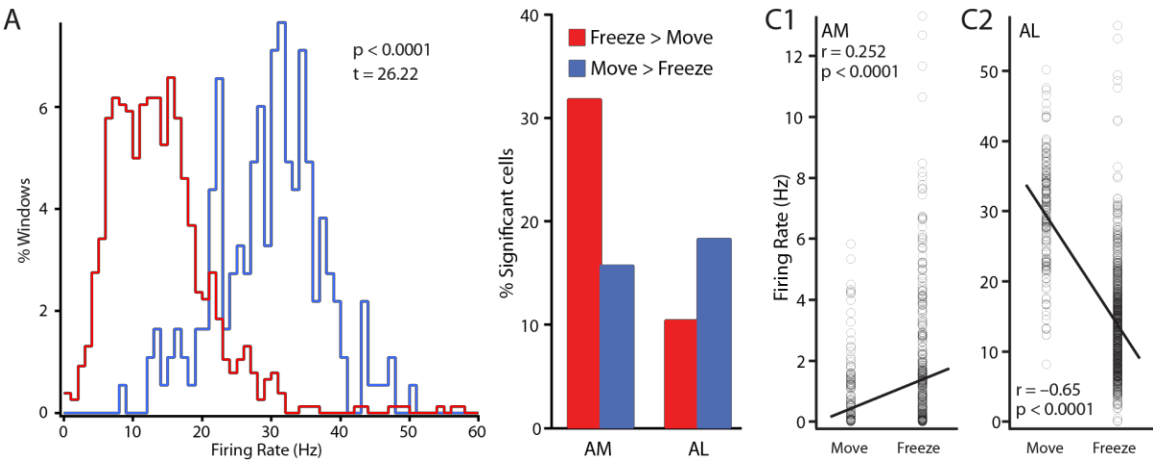

Figure 5.8. Analysis of fluctuations in firing rates during movement vs. freezing. (**A**) Frequency distributions of firing rates during 0.5 sec windows of freezing (red) or movement (blue) for a BNST-AL cell. (**B**) Incidence of BNST-AM (left) and AL (right) cells with significantly higher firing rates during freezing (red) or movement (blue). (**C**) Correlation between motor activity (freezing = 1; movement = 0) and firing rate for individual BNST-AM (**C1**) and AL (**C2**) cells.

Although prior lesion studies suggest that BNST plays an important role in the genesis of contextual freezing, it remains possible that the differences in firing rates described above do not relate to the affective state of the rats but to another factor such as proprioceptive feedback. To address this possibility, we compared the spontaneous firing rates of BNST-AL and AM neurons while the animals were in a neutral transfer cage prior to placement in Context A (10 min epochs). In this environment, rats were generally active. Periods of immobility were almost always followed by a shift in their behavioral state to slow-wave sleep (SWS). This shift was easy to identify because it coincided with a dramatic increase in the power of large amplitude slow oscillations ≤ 4 Hz in the local field potentials.

Thus, using the same approach as in the above, we compared firing rates during movement vs. immobility, but excluding periods of overt SWS. Respectively 33.3% and 39.3% of BNST-AL and AM neurons were found to have signifi-

cantly different firing rates in the two conditions. However, the proportion of cells with higher firing rates in one condition or the other did not differ significantly (Fisher exact: AM, $p = 0.23$; AL, $p = 0.43$).

5.4) *Discussion*

The experiments undertaken in the third AIM examined the behavior of anterior BNST neurons during cued and contextual fear. The findings point to a high level of region specific activity within the BNST-AL and AM in relation to learned fear, raising the possibility that they exert opposite influences on fear output networks. Furthermore, the stronger recruitment of BNST-AM neurons during contextual relative to cued fear may account for the BNST's selective involvement in contextual fear conditioning. The findings reflect the regional heterogeneity within the anterior BNST. Indeed, the present study revealed that BNST-AL and AM neurons display a different activity profile in relation to learned fear. First, during cued fear conditioning, BNST-AL neurons acquired *inhibitory* responses to the CS (Off-cells). Two days later, during the recall test, the proportion of Off-cells remained high but an additional subset of cells developed positive responses to the CS (On-cells). In contrast, the CS responsiveness of BNST-AM neurons did not change during training. However, during the recall test two days later, we observed a large increase in the incidence of cells with *excitatory* responses to the CS. Importantly, BNST-AL and AM neurons displayed an opposite activity profile in relation to contextual fear. Indeed, when rats were exposed to the training context the day after fear conditioning, a third of BNST-AM neurons fired at significantly *higher* rates during freezing than movement.

Few BNST-AM cells showed the opposite behavior. By contrast, in BNST-AL, neurons with *lower* firing rates during freezing prevailed, consistent with the pattern of CS responsiveness described above.

Chapter VI

General Discussion

6.1) *Rationale*

Prior tract-tracing studies have shown puzzling variations in the path followed by CeA axons to the brain stem (Dong et al. 2001a; Krettek and Price 1978b; Price and Amaral 1981; Sun and Cassell 1993; Veinante and Freund-Mercier 2003). Although many CeA axons reach the brain stem directly via the ventral amygdalofugal pathway, others follow the stria terminalis over its entire course. Thus they first course caudally, then arch dorsally and rostrally along the lateral aspect of the thalamus, and later curve ventrally and caudally to merge with axons of the ventral amygdalofugal pathway. They also synapse onto BNST neurons, which receive massive inputs from BL sources. These anatomical findings lead us to the idea that the BNST could play a here-to-for unknown role in fear output behaviors.

6.2) *Timing of interactions between CeM and BNST*

Our first study was undertaken to shed light on the functional interactions between CeM and BNST neurons with a particular emphasis on the relative timing of their outputs to the brain stem. The interest of this question stems from earlier findings suggesting that despite having similar connections and anatomical properties, CeM and BNST play different roles in regulating behavior. Our results point to an unexpected level of coordination in the timing of BNST and CeM outputs to the brain stem, relative to BL inputs. Below, we consider the significance of these findings in light of previous anatomical and behavioral studies on the role of the extended amygdala.

Consistent with this, our analysis of brain stem–evoked antidromic response latencies has shown that CeA output neurons fall into two classes, with short or long conduction times to the brain stem. The rarity of CeA cells with long antidromic response latencies in rats prepared with lesions of the stria terminalis strongly suggests that the neurons with long conduction times correspond to the subset of CeA cells whose axons reaches the brain stem via the stria terminalis. The net consequence of this path heterogeneity is that some CeA impulses reach their brain stem targets quickly, in ~10 ms, whereas others take around three times longer.

What could be the significance of this peculiar arrangement? One possibility is that it serves no special purpose. According to this view, the path heterogeneity would reflect a developmental oddity where some CeM cells, subjected to conflicting chemotaxic cues, would be lured into the stria terminalis, whereas others would merge with the ventral amygdalofugal pathway. However, a second possibility, the one we favor, is that this arrangement serves to synchronize CeA and BNST outputs to the brain stem when they are activated by BL inputs. Synchronization of CeM and BNST impulses to the brain stem would likely enhance the postsynaptic impact of each input.

Consistent with this possibility, we observed that the latency of peak BL-evoked responses was longer in BNST cells, by ~20 ms, than seen in CeA cells. This difference closely approximated the conduction delay introduced by lengthening the path of CeM axons to the brain stem via the stria terminalis. Thus by lengthening the path of some CeM axons to the brain stem, the arrival of BL-

driven CeM impulses would be delayed, allowing for synchronization of BNST and CeM impulses on their targets. This idea is further supported by a previous anatomical study showing that the same BL neurons that project to CeM also contribute axon collaterals to the BNST (Smith & Millhouse 1985).

However, there is a third possible interpretation for our findings. This view assumes that BNST and CeA neurons with slow versus fast conduction times to the brain stem do not converge on the same brain stem neurons. Although the tract-tracing data indicates that the brain stem targets of CeA and BNST neurons overlap extensively at a macroscopic level (Dong & Swanson 2004, 2006a–c; Dong et al. 2000; Holstege et al. 1985; Hopkins & Holstege 1978; Veening et al. 1984), it remains to be shown, at the single cell level, whether convergence occurs for inputs originating from all three cell groups. For instance, it is conceivable that fast-conducting CeA neurons contact brain stem neurons involved in the rapid mediation of short-lived fear responses. In contrast, slow conducting CeM neurons and BNST cells might contact brain stem targets that are involved in more persistent fear responses. An important challenge for future studies will be to compare the brain stem projection sites of BNST and CeM neurons with slow or fast conduction times to the brain stem.

A puzzling difference between CeM and BNST neurons evidenced in this study was that BL stimuli evoked a much longer period of increased firing probability in BNST than CE cells. Although differences in the electroresponsive properties of CeM and BNST neurons might have contributed to this effect, it is also possible that BL stimuli engaged contrasting polysynaptic influences. In particu-

lar, CeM neurons receive a strong GABAergic input from intercalated amygdala neurons (Paré and Smith 1993) that also receive inputs from BL (Royer et al. 1999). The excitation of ITC neurons by BL inputs was previously shown to generate a rapid feed-forward inhibition in CeM neurons, limiting the duration of BL-evoked excitatory postsynaptic potentials (EPSPs) (Royer et al. 1999). In addition, BL projects to the medial prefrontal cortex (Krettek & Price 1977) that in turn projects to BNST (Vertes 2004). Thus the excitation of BNST neurons by BL inputs may have been prolonged via the activation of the medial prefrontal cortex.

6.2.1) *Behavioral significance of path heterogeneity*

Our analyses of BL-evoked response latencies and conduction times to the brainstem argue for a tight temporal coordination between CeM and BNST outputs. However, this view does not fit with the lesion and pharmaco-behavioral studies reviewed in the introduction that stress the different functions of CeM and BNST. However, it remains that some effects of BNST and CeM lesions overlap. For instance, ibotenic acid lesions of BNST (Gray et al. 1993) and CeM (Van de Kar et al. 1991) attenuate the increase in corticosterone associated with the expression of contextually conditioned fear. CeM and BNST lesions were also reported to attenuate behaviors that are thought to depend on parallel projections of these structures to the brain stem. For instance, it was observed that the expression of contextual conditioned freezing responses is attenuated by both CeM and BNST lesions (Goosens and Maren 2001; Gray et al. 1993; Sullivan et al. 2004; Van de Kar et al. 1991). Moreover, CeM and anterior BNST lesions pre-

vent the pain-induced increase in vocalization seen following exposure to noxious electrical stimuli (Crown et al. 2000). Both of these effects are thought to depend on parallel projections of CeM and BNST to the PAG: the ventral PAG for freezing responses (LeDoux et al. 1988) and the dorsal PAG for the pain-induced increase in vocalization (Crown et al. 2000; McLemore et al. 1999).

6.2) *Spontaneous activity of BNST neurons during the sleep-wake cycle*

Even in the absence of sensory stimulation, the spontaneous activity of the brain is not random. Rhythmic population events, measurable in the extracellular space as currents, emerge from complex interactions between the intrinsic properties of neurons and the architecture of the network in which they are embedded. Rhythms of various frequencies occur in different brain regions and these oscillations change depending on the behavioral state.

The importance of these oscillations derives from the fact that neuronal events underlying cognitive activity, be it memory, emotional expression or sensory perception, are embedded in these endogenous population rhythms. In other words, the study of oscillations and coding in large neuronal ensembles are inextricable. Moreover, during sleep, when the brain is largely disconnected from the outside world, neurons generate a variety of oscillations and synchronized population bursts that are believed to play a critical role in memory consolidation. Finally, because related parts of the brain tend to display similar oscillations, the analysis of spontaneous oscillatory activity can reveal functional kinship among brain structures.

This study focuses on the spontaneous oscillatory activity displayed by neurons in the bed nucleus of the stria terminalis. The BNST is a poorly understood brain region that has been implicated in a variety of functions, most relating to negative affect and stress. While the structure and connectivity of BNST is well known, its physiology has received very little attention. Thus, as a first step toward understanding the basic physiological organization of BNST, the present study characterizes the spontaneous activity of neurons in its anteromedial (AM) and anterolateral (AL) portions during different states of vigilance.

We found that the spectral composition fluctuated in a state-dependent manner. The findings are similar to LFP frequencies observed in many regions of the brain during SWS, REM and W. However it is important to note that, the various LFP rhythms recorded in BNST-A were not volume conducted from neighboring structures. Indeed, a substantial proportion of BNST-AL and AM cells showed significant modulation of unit activity in the delta, theta, and gamma bands.

6.3) *Activity of BNST neurons in animals undergoing differential fear conditioning*

We have studied the behavior of anterior BNST neurons during cued and contextual fear. The interest of this question stems from earlier work indicating that BNST and CeA, despite forming similar connections with the basolateral amygdala (BLA) and brainstem fear effectors, are differentially involved in contextual vs. cued fear. Surprisingly, while we observed regional differences in

BNST activity in relation to fear, the pattern of results was similar for contextual and cued fear. The significance of these findings is considered below.

There is consensus that BNST is involved in the genesis of contextual, but not cued fear. Reversible inactivation (Walker and Davis 1997) as well as electrolytic (Gewirtz et al. 1998; Sullivan et al. 2004; Waddell et al. 2006; Luyten et al. 2011) or neurotoxic (LeDoux et al. 1988; Hammack et al. 2004; Duvarci et al. 2009) lesions of BNST impair the expression of contextual but not cued fear, unless the CS is very long (Waddell et al. 2006) or the temporal relationship between the CS and US is ambiguous (Walker et al. 2009). However, other studies suggest that BNST activity, while not required for generating learned fear to cues, exerts a tonic inhibitory influence on fear output networks. Indeed, intra-BNST infusions of muscimol *enhance* fear potentiated startle (Meloni et al. 2006). Moreover, presentation of a fear-eliciting CS together with a conditioned inhibitor *increase* fos expression in BNST relative to animals only presented with the CS (Campeau et al. 1997). Last, intra-BNST infusions of calcitonin gene-related peptide (CGRP) enhance startle and increase Fos expression in CeA (Sink et al. 2011). However, a patch-clamp study found that CGRP potentiates GABAergic inhibition in neurons of BNST-AL (Gungor and Paré 2012), the BNST region receiving CGRP inputs from the parabrachial nucleus (Gustafson and Greengard 1990; Dobolyi et al. 2005). Since most BNST neurons are GABAergic (Esclapez et al. 1993; Poulin et al. 2009), these results suggest the startle enhancement produced by intra-BNST infusions of CGRP is due to the inhibition of BNST-AL neurons and consequent disinhibition of CeA.

6.3.2) *Activity of BNST-neurons in relation to cued and contextual fear*

Overall, the findings reviewed above support the view that BNST exerts a dual influence over fear expression. On the one hand, BNST supports contextual fear; on the other, there is evidence that BNST, most likely its anterolateral region, exerts an inhibitory influence over fear output networks. As described below, we propose that this apparent contradiction reflects regional heterogeneity in the anterior BNST. Indeed, the present study revealed that BNST-AL and AM neurons display a different activity profile in relation to learned fear. First, during cued fear conditioning, BNST-AL neurons acquired *inhibitory* responses to the CS (Off-cells). Two days later, during the recall test, the proportion of Off-cells remained high but an additional subset of cells developed positive responses to the CS (On-cells). In contrast, the CS responsiveness of BNST-AM neurons did not change during training. However, during the recall test two days later, we observed a large increase in the incidence of cells with *excitatory* responses to the CS. Importantly, BNST-AL and AM neurons displayed an opposite activity profile in relation to contextual fear. Indeed, when rats were exposed to the training context the day after fear conditioning, a third of BNST-AM neurons fired at significantly *higher* rates during freezing than movement. Few BNST-AM cells showed the opposite behavior. By contrast, in BNST-AL, neurons with *lower* firing rates during freezing prevailed, consistent with the pattern of CS responsiveness described above.

These findings point to regional differences in the activity of BNST-AL and

AM in relation to learned fear, raising the possibility that they exert opposite influences on fear output networks. Several factors likely underlie these differences, including regionally heterogeneous amygdala projections to BNST as well as the intrinsic BNS network. Indeed, the amygdala sends strong but neurochemically diverse projections to BNST: GABAergic/peptidergic inputs from CeA and glutamatergic inputs from BLA (Krettek and Price 1978b; Dong et al. 2001a; McDonald, 2003). Importantly, CeA contributes stronger projections to BNST-AL than AM (Dong et al. 2001a). Conversely, a major component of BNST-AL, the oval nucleus, is largely devoid of BLA inputs (Dong et al. 2001a). In addition, a recent in vitro study on the intrinsic connections of BNST reported that BNST-AL neurons receive inhibitory inputs from other BNST neurons (Turesson et al. 2013). Thus, CS-related BLA inputs might excite BNST cells that send GABAergic projections to neurons of the oval nucleus, causing a feedforward inhibition. This inhibition of BNST-AL neurons might be reinforced by CeA inputs, which are much stronger to BNST-AL than AM (Dong et al. 2001a).

Consistent with the above, there is a correspondence between the CS responsiveness of neurons in the lateral (CeL) and medial (CeM) sectors of CeA and BNST. In particular, most CS responsive CeM neurons exhibit positive responses to the CS (Ciocchi et al. 2010; Duvarci et al. 2011), as in BNST-AM. In contrast, as in BNST-AL, CeL responses to the CS are heterogeneous, with different CeL neurons exhibiting inhibitory or excitatory responses (Ciocchi et al. 2010; Duvarci et al. 2011). Perhaps not coincidentally, the incidence of CeL Off-cells does not increase during training, but after a consolidation period (Duvarci

et al. 2011). In parallel, an inflation of CS-evoked responses develops in BLA (Amano et al. 2011). At present, the cellular interactions leading to these time-dependent changes in CS responsiveness remain unclear. However, given the strong interconnections existing between BLA, CeA, and BNST neurons, a causal relation is likely. Also, considering the dramatic impact of medial prefrontal lesions on the expression of learned fear (Sierra-Mercado et al. 2011) and the preferential innervation of BNST-AM by prelimbic afferents (reviewed in McDonald 1999), it is probable that prefrontal inputs also play a role.

6.3.3) *Preferential BNST contribution to contextual fear*

If BNST-AM and AL neurons show the same differential activity profile in relation to cued and contextual fear, why do lesion and inactivation studies consistently conclude that BNST participates in contextual but not cued fear? This apparent contradiction can be resolved if we postulate that BNST-AL and AM exert opposite influences over fear output networks, a notion supported by the reciprocal activity profile evidenced here. Based on the fact that CGRP enhances fear-potentiated startle (Sink et al. 2011) while inhibiting BNST-AL neurons (Gungor and Paré 2012), the following model assumes that the reduced activity seen in a proportion of BNST-AL neurons during high fear states causes a disinhibition of CeA fear output neurons. In contrast, the increased activity observed in BNST-AM, much like the CS-On responses of CeM neurons (Ciocchi et al. 2010; Duvarci et al. 2011), would drive behavioral freezing via the vlPAG. Indeed, our tracing experiments indicate that PAG projecting neurons are much

more numerous in BNST-AM than AL (SC Lee and D Paré, unpublished observations; however, see Zahm et al. 2011).

In light of the above, given that lesion and infusion techniques lack the resolution to affect BNST-AL and AM independently, the net outcome of complete BNST lesions or inactivations should be a function of the imbalance in responsiveness between the two regions. If the two regions show similar levels of responsiveness, as seen in cued fear, little or no effect should be observed. In contrast, if one of the two regions shows a higher level of activity, as seen in relation to contextual fear, then complete BNST lesions should alter fear expression. An important challenge for future experiments will be to test this model with spatially selective manipulations of different regions of the anterior BNST.

In closing, it should be mentioned that opposite to the above, a recent study (Kim et al. 2013) concluded that the BNST-AL and AM exert anxiogenic and anxiolytic influences, respectively. This view was mainly based on the outcome of optogenetic manipulations thought to allow selective alterations in the activity of the two BNSTa sectors. For instance, optogenetic activation or inhibition of BLA inputs to BNST-AM was seen to reduce or enhance various measures of anxiety, respectively (Kim et al. 2013). However, BLA heavily projects to nucleus accumbens (nAcc; Krettek and Price 1978b), which is immediately rostral to BNST, and a prior study reported that optogenetic activation of BLA inputs to nAcc facilitates reward seeking (Stuber et al. 2011). Since BLA inputs to nAcc course through and in the immediate vicinity of BNST, it

is possible that light stimuli in BNST also affected BLA inputs to nAcc. In keeping with this, Kim et al. (2013) reported that intra-BNST infusions of ionotropic glutamate receptor antagonists reduced anxiety. This finding is in apparent contradiction with the results of the optogenetic manipulations. Indeed, the main glutamatergic input to BNST arises in BLA and its projections focus on BNST-AM while avoiding much of BNST-AL (Krettek and Price 1978b; Dong et al. 2001a). Therefore, if BLA inputs to BNST-AM supported anxiolysis, one would have expected the opposite effect. Additional experiments will be required to settle these issues.

6.5) *Final Conclusion*

The experiments presented in this thesis were undertaken to shed light on the mechanisms underlying role of BNST the processing of fearful memories. Unlike previous studies, we found that the BNST does participate in the processing of conditioned fear. The conclusions from the Aim #1 indicate that the BLA is in a position to coordinate the outputs of CeM and BNST neurons in such a way as to maximize their postsynaptic impact on brainstem targets. The findings from Aim #3 show a clear increase in the activity of BNST-AM and –AL cells excited by the CS+ during recall testing. Furthermore BNST-AM neurons also show enhanced activity during contextual freezing. It is well known that the largest excitatory input to the BNST-AM originates from the BL (Dong et al. 2001a). Tying together the results of those two Aims, it is possible that excitatory BL inputs could activate downstream projecting neurons in BNST-AM to drive freezing behavior during the recall testing phase of fear conditioning. A second

possibility for heightened BNST activity during fear recall and context testing calls into play the important relationship between context and fear recall. Context has a profound effect on the recall of associative fear memory. Substantial behavioral evidence indicates that fear recall in which a CS is presented in the absence of a US is a product of the inhibition of fear expression. Rather than being an erasure of memory it represents a new learning of the CS meaning (Bouton 1993, Quirk 2002, Rescorla 2001). Just like with the original association, this learning is highly context specific. Indeed recall testing is thought to be more context specific than fear learning (for review see Bouton 2004). As such, in both context testing and recall testing the subject is processing contextual information in an environment where fear is expected but not received. BNST activity during this period may reflect the processing of this information.

References

Adamec R. 1989. The relationship between the amygdala and bed nucleus of the stria terminalis in the cat: an evoked potential and single cell study. *Behav Neural Biol* **52**:295-320.

Aggleton JP. 2000. The Amygdala: a functional analysis. Oxford University Press. 2nd Edition 690 pp.

Alheid GF, Heimer L. 1988. New perspectives in basal forebrain organization of special relevance for neuropsychiatric disorders: the striatopallidal, amygdaloid, and corticopetal components of substantia innominata. *Neuroscience* **27**: 1-39.

Alheid G, de Olmos JS, Beltramino CA. 1995. Amygdala and extended amygdala. In: Paxinos, G. (Ed.) The Rat Nervous System Academic Press New York : 495 – 578.

Amaral DG, Price JL, Pitkanen A, Carmichael ST. 1992. Anatomical organization of the primate amygdaloid complex. In Aggleton, JP (ed.) The Amygdala: Neurobiological Aspects of Emotion, Memory, and Mental Dysfunction. Wiley-Liss, New York: 1–66.

Anglada-Figueroa D, Quirk GJ. 2005 Lesions of the basal amygdala block expression of conditioned fear but not extinction. *J Neurosci* **25**: 9680-9685.

Baxter MG, Murray EA. 2002. The amygdala and reward. *Nature Reviews Neuroscience* **3**: 563-573.

Biederman J, Hirshfeld-Becker DR, Rosenbaum JF, Herot C, Friedman D, Snidman N. 2001. Further evidence of association between behavioral inhibition and social anxiety in children. *Am J Psychiatry* **158**: 1673–1679.

Bishop SJ. 2007 Neurocognitive mechanisms of anxiety: an integrative account. *Trends Cogn Sci* **11**: 307–316.

Blair HT, Schafe GE, Bauer EP, Rodrigues SM, Ledoux JE. 2001. Synaptic plasticity in the lateral amygdala: a cellular hypothesis of fear conditioning. *Learning and Memory* **8**: 229–242.

Blanchard DC, Blanchard RJ. 1972. Innate and conditioned reactions to threat in rats with amygdaloid lesions. *J Comp Physiol Psychol* **81**: 281–290.

Blanchard RJ, Blanchard DC, Agullana R, Weiss SM. 1991. Twenty-two kHz alarm cries to presentation of a predator, by laboratory rats living in visible burrow systems. *Physiol Behav* **50**: 967-972.

Bouton ME**.** 1993. Context, time, and memory retrieval in the interference paradigms of Pavlovian learning. *Psychol Bull* **114**: 80–99.

Bouton ME. 2004*.* Context and Behavioral Processes in Extinction. *Learning and Memory* **11**: 485-494.

Brown S, Schäfer A. 1888. An investigation into the functions of the occipital and temporal lobes of the monkey's brain. *Philos Trans R Soc London Ser B* **179**: 303–27.

Bupesh M, Abellán A, Medina L. 2011. Genetic and experimental evidence supports the continuum of the central extended amygdala and a mutiple embryonic origin of its principal neurons. *J Comp Neurol* **519**: 3507-31.

Campeau S, Davis M. 1995. Involvement of the central nucleus and basolateral complex of the amygdala in fear conditioning measured with fear-potentiated startle in rats trained concurrently with auditory and visual conditioned stimuli. *J Neurosci* **15**: 2301-2311.

Campeau S, Falls WA, Cullinan WE, Helmreich DL, Davis M, Watson SJ. 1997. Elicitation and reduction of fear: behavioural and neuroendocrine indices and brain induction of the immediate-early gene c-fos.
Neuroscience **78**:1087-104.

Carobrez AP, Schenberg LC, Graeff FG. 1983. Neuroeffector mechanisms of the defense reaction in the rat. *Physiol Behav.* **31**: 439-44.

Cassell MD, Gray TS. 1989. The amygdala directly innervates adrenergic (C1) neurons in the ventrolateral medulla in the rat. *Neuroscience* **97**: 163–168.

Cassell MD, Freedman LJ, Shi C. 1999. The intrinsic organization of the central extended amygdala. *Ann N Y Acad Sci* **29**; 217-41.

Chen HC, Chen DY, Chen CC Liang KC. 2004. Pre- and post-training infusion of prazosin into the bed nucleus of the stria terminalis impaired acquisition and retention in a Morris water maze task. *Chinese Journal of Physiology* **47**: 49–59.

Ciocchi S, Herry C, Grenier F, Wolff SB, Letzkus JJ, Vlachos I, Ehrlich I, Sprengel R, Deisseroth K, Stadler MB, Müller C, Lüthi A. 2010. Encoding of conditioned fear in central amygdala circuits. *Nature* **468:** 277-282.

Cohen H, Zohar J, Gidron Y, Matar MA, Belkind D, Loewenthal U, Kozlovsky N, Kaplan Z. 2006. Blunted HPA axis response to stress influences susceptibility to posttraumatic stress response in rats. *Biol Psychiatry* **59**:1208-18.

Crown ED**,** King TE, Meagher MW, Grau JW. 2000. Shock-induced hyperalgesia: III. Role of the bed nucleus of the stria terminalis and amygdaloid nuclei. *Behav Neurosci* **114**: 561–573.

Darwin C. 1965. The Expression of Emotion in Man and Animals. University of Chicago Press. Chicago [1872].

Dave AS, Margoliash D. 2000. Song Replay During Sleep and Computational Rules for Sensorimotor Vocal Learning. *Science* **290**: 812–815.

Davis M. 1997. Neurobiology of fear responses: the role of the amygdala. *J Neuropsy Clin Neurosci* **9**: 382–402.

Davis M. 2000. The role of the amygdala in conditioned and unconditioned fear and anxiety. In: The amygdala. Aggleton JP, editor. New York: Oxford University Press 213–287.

Davis M, Walker DL, Lee Y. 1997. Roles of the amygdala and bed nucleus of the stria terminalis in fear and anxiety measured with the acoustic startle reflex. Possible relevance to PTSD. *Ann NY Acad Sci* **821**: 305-331.

Davis M, Walker DL, Miles L, Grillon C. 2010. Phasic vs sustained fear in rats and humans: role of the extended amygdala in fear vs anxiety. *Neuropsychopharmacology* **35**:105-35.

de Olmos JS, Heimer L. 1999. The concepts of the ventral striatopallidal system and extended amygdala. *Ann N Y Acad Sci* **877**: 1-32.

Delgado J MR (1968) Physical Control of the Mind: Towards a Psychocivilized Society. Harper and Row: New York.

Desai SA, Rolston JD, Guo L, Potter SM. 2010. Improving impedance of implantable microwire multi-electrode arrays by ultrasonic electroplating of durable platinum black. *Front Neuroeng* **3**:5.

Diekelmann S, Born J. 2010. The memory function of sleep. *Nat Rev Neurosci* **11**:114-26.

Dobolyi A, Irwin S, Makara G, Usdin TB, Palkovits M. 2005. Calcitonin gene related peptide containing pathways in the rat forebrain. *J Comp Neurol* **489:** 92-119.

Dong HW, Petrovich G, Swanson LW. 2000.Organization of projections from the juxtacapsular nucleus of the BST: a PHAL study in the rat. *Brain Res* **859**: 1–14.

Dong HW, Petrovich GD, Swanson LW. 2001a. Topography of projections from amygdala to bed nuclei of the stria terminalis. *Brain Res Rev* **38**: 192-246.

Dong HW, Petrovich GD, Watts AG, Swanson LW. 2001b. Basic organization of projections from the oval and fusiform nuclei of the bed nuclei of the stria terminalis in adult rat brain. *J Comp Neurol* **436**: 430-455.

Dong HW, Swanson LW. 2003. Projections from the rhomboid nucleus of the bed nucleus of the stria terminalis: implications for cerebral hemisphere regulation of ingestive behaviors. *J Comp Neurol* **463:** 795-9.

Dong HW, Swanson LW. 2004. Organization of axonal projections from the anterolateral area of the bed nuclei of the stria terminalis. *J Comp Neurol* **468**: 277-98.

Dong HW, Swanson LW. 2006a. Projections from bed nuclei of the stria terminalis, anteromedial area: cerebral hemisphere integration of neuroendocrine, autonomic, and behavioral aspects of energy balance. *J Comp Neurol* **494**: 142-78.

Dong HW, Swanson LW 2006b Projections from bed nuclei of the stria terminalis, dorsomedial nucleus: implications for cerebral hemisphere integration of neuroendocrine, autonomic, and drinking responses. *J Comp Neurol* **494**: 75-107.

Dong HW, Swanson LW. 2006c. Projections from bed nuclei of the stria terminalis, dorsomedial nucleus: implications for cerebral hemisphere integration of neuroendocrine, autonomic, and drinking responses. *J Comp Neurol* **494:** 75-107.

Dunn JD. 1987. Plasma corticosterone responses to electrical stimulation of the bed nucleus of the stria terminalis. *Brain Res* **407**: 327–331.

Duvarci S, Bauer EP, Paré D. 2009. The bed nucleus of the stria terminalis mediates inter-individual variations in anxiety and fear. *J Neurosci* **29:** 10357-10361.

Duvarci S, Popa D, Paré D. 2011. Central amygdala activity during fear conditioning. *J Neurosci* **31:** 289-294.

Egli RE, Winder DG. 2003. Dorsal and ventral distribution of excitable and synaptic properties of neurons of the bed nucleus of the stria terminalis. *J Neurophysiol* **90**: 405-14.

Fanselow MS. 1980. Conditioned and unconditional components of post-chock freezing. *Pavlov J Biol Sci* **15**: 177-82.

Fendt M, Fanselow MS. 1999. The neuroanatomical and neurochemical basis of conditioned fear. *Neurosci Biobehav Rev* **23**: 743–760.

Fendt M, Endres T, Apfelbach R. 2003. Temporary inactivation of the bed nucleus of the stria terminalis but not of the amygdala blocks freezing induced by trimethylthiazoline, a component of fox feces. *J Neurosci* **23**: 23–28.

Ferguson JE Boldt C Redish AD. 2009. Creating low-impedance tetrodes by electroplating with additives. *Sens Actuators A Phys* **156**: 388-393.

Frank NP. 2008. General anaesthesia: from molecular targets to neuronal pathways of sleep and arousal. *Nat Rev Neurosci* **9**: 370-86.

Freud, S. 1900. Die Traumdeutung [The interpretation of dreams]. In: Gesammelte Werke. Vol. 2/3. Frankfurt: S. Fischer; 1998.

Gale GD, Anagnostaras SG, Godsil BP, Mitchell S, Nozawa T, Sage JR, Wiltgen B, Fanselow MS. 2004. Role of the basolateral amygdala in the storage of fear memories across the adult lifetime of rats. *J Neurosci* **24**: 3810-15.

García-López M, Abellán A,Legaz I, Rubenstein JLR, Puelles L, Loreta Medina L. 2008. Histogenic compartments of the mouse centromedial and extended amygdala based on gene expression patterns during development *J Com Neurol* **506**: 46-74.

Gerren RA, Weinberger NM. 1983. Long term potentiation in the magnocellular medial geniculate nucleus of the anesthetized cat. *Brain Res* **265**: 138-142.

Gewirtz JC, McNish KA, Davis M. 1998. Lesions of the bed nucleus of the stria terminalis block sensitization of the acoustic startle reflex produced by repeated stress, by not fear-potentiated startle. *Prog Neuropsychopharmacol Biol Psychiatry*. **22**: 625-48.

Goosens KA, Maren S. 2001. Contextual and auditory fear conditioning are mediated by the lateral, basal, and central amygdaloid nuclei in rats. *Learn Mem* **8**: 148–155.

Goosens KA, Maren S. 2003. Pretraining NMDA receptor blockade in the

basolateral complex, but not the central nucleus, of the amygdala prevents savings of conditional fear. *Behav Neurosci* 117: 738 –750.

Goswami S, Samuel S, Sierra OR, Cascardi M, Paré D. 2012. A rat model of post-traumatic stress disorder reproduces the hippocampal deficits seen in the human syndrome. *Front Behav Neurosci.***6**: 3-8.

Gray TS, Carney ME, Magnuson DJ. 1989. Direct projections from the central amygdaloid nucleus to the hypothalamic paraventricular nucleus: possible role in stress-induced adrenocorticotropin release. *Neuroendocrinology* **50**: 433–446.

Van der Helm E, Walker MP. 2009. Overnight therapy? The role of sleep in emotional brain processing. *Psychological Bulletin* **135**: 731–748.

Graves LA, Heller EA, Pack AI, Abel T. 2003. Sleep deprivation selectively impairs memory consolidation for contextual fear conditioning. *Learn Mem.* **10**: 168-76.

Gray TS, Piechowski RA, Yracheta JM, Rittenhouse PA, Bethea CL, Van de Kar LD. 1993. Ibotenic acid lesions in the bed nucleus of the stria terminalis attenuate conditioned stress-induced increases in prolactin, ACTH and corticosterone. *Neuroendocrinology* **57**: 517–524.

Guillemin R, Rosenberg B. 1955. Humoral hypothalamic control of anterior pituitarya study with combined tissue cultures. *Endocrinology* **57**: 599–607.

Gungor NZ, Paré D. 2012. In vitro study of CGRP effects suggests that BNST-AL neurons exert an anxiolytic influence. *Soc for Neurosci abstract* 603.16.

Gustafson EL, Greengard P. 1990. Localization of DARPP-32 immunoreactive neurons in the bed nucleus of stria terminalis and central nucleus of amygdala: co distribution with axons containing tyrosine hydroxylase, vasoactive intestinal polypeptide, and calcitonin gene related peptide. *Exp Brain Res* **1990:** 447-458.

Hammack SE, Richey KJ, Watkins LR, Maier SF. 2004. Chemical lesion of the bed nucleus of the stria terminalis blocks the behavioral consequences of uncontrollable stress. *Behav Neurosci* **118**: 443-8.

Hammack SE, Mania I, Rainnie DG. 2007. Differential expression of intrinsic membrane currents in defined cell types of the anterolateral bed nucleus of the stria terminalis. *J Neurophysiol* **98**:638-56.

Han ZS, Ju G. 1990. Effects of electrical stimulation of the central nucleus of the amygdala and the lateral hypothalamic area on the oval nucleus of the bed nuclei of the stria terminalis and its adjacent areas in the rat. *Brain Res.* **536**: 56-62.

Hazra R, Guo JD, Ryan SJ, Jasnow AM, Dabrowska J, Rainnie DG. 2011. A transcriptomic analysis of type I-III neurons in the bed nucleus of the stria terminalis. *Mol Cell Neurosci* **46**: 699-709.

Herman JP, Cullinan WE, Watson SJ. 1994. Involvement of the bed nucleus of the stria terminalis in tonic regulation of paraventricular hypothalamic CRH and AVP mRNA expression. *J Neuroendocrinol* **6**: 433-442.

Herman JP, Cullinan WE. 1997. Neurocircuitry of stress: central control of the hypothalamo-pituitary-adrenocortical axis. *Trends Neurosci* **20**: 78-84.

Herman JP, Figueiredo H, Mueller NK, Ulrich-Lai Y, Ostrander MM, Choi DC, Cullinan WE. 2003. Central mechanisms of stress integration: hierarchical circuitry controlling hypothalamo-pituitary-adrenocortical responsiveness. *Front Neuroendocrinol* 24: 151–180.

Herman JP, Ostrander MM, Mueller NK, Figueiredo H. 2005. Limbic system mechanisms of stress regulation: hypothalamo-pituitary-adrenocortiacal axis. *Prog Neuropsychoparmacol Biol Psychiatry* **29**: 1201-13.

Herman JP, Cullinan WE, Watson SJ. 2006. Involvement of the bed nucleus of the stria terminalis in tonic regulation of of paraventricular hypothalamic CRH and AVP mRNA expression. *J Neuroendocrin* **6**: 433-442.

Herry C, Ciocchi S, Senn V, Demmou L, Muller C, Luthi A. 2008. Switching on and off fear by distinct neuronal circuits. *Nature* **454**: 600-6.

Hitchcock JM, Davis M. 1987. Fear-potentiated startle using an auditory conditioned stimulus: effect of lesions of the amygdala. *Physiol Behav* **39**: 403-8.

Hitchcock JM, Davis M. 1991. The efferent pathway of the amygdala involved in conditioned fear as measured with the fear-potentiated startle paradigm. *Behav Neurosci* **105**: 826–842.

Holstege G, Meiners L, Tan K. 1985. Projections of the bed ucleus of the stria terminalis to the mesencephalon, pons, and medulla oblongata. *Exp Brain Res* **58**: 379-91.

Hopkins DA, Holstege G. 1978. Amygdaloid projections to the mesencephalon, pons and medulla oblongata in the cat. *Exp Brain Res* **32**: 529 –547.

Iwata J, LeDoux JE, Meeley MP, Arneric S, Reis DJ. 1986. Intrinsic neurons in the amygdaloid field projected to by the medial geniculate body mediate emotional responses conditioned to acoustic stimuli. *Brain Res* **383**: 195– 214.

Iwata J, Chida K, LeDoux JE. 1987. Cardiovascular responses elicited by stimulation of neurons in the central amygdaloid nucleus in awake but not anesthetized rats resemble conditioned emotional responses. *Brain Res* **418**: 183-188.

Jankord R, Herman JP. 2008. Limbic regulation of hypothalamo-pituitary-adrenocortical function during acute and chronic stress. *Ann N Y Acad Sci* **1148**:64-73.

Johansen JP, Cain CK, Ostroff LE, LeDoux JE. 2011. Molecular mechanisms of fear learning and memory. *Cell* **147**: 509-524.

Jolkkonen M, Pikkarainen S, Kemppainen S, Pitkänen A. 2001. Interconnectivity between the amygdaloid complex and the amygdalostriatal transition area: a PHA-L study in rat. *J Comp Neurol* **431**: 39-58.

Johnston JB. 1923. Further contributions to the study of the evolution of the forebrain. *J Comp Neurol* **35**: 337–481.

Ji J, Maren S. 2007. Hippocampal involvement in contextual modulation of fear extinction. *Hippocampus* **17**: 749–758.

Jimenez SA, Maren S. 2009. Nuclear disconnection within the amygdala reveals a direct pathway to fear. *Learn Mem* **16:** 766-768.

Ju G, Swanson LW. 1989a. Studies on the cellular architecture of the bed nuclei of the stria terminalis in the rat: I. Cytoarchitecture. *J Comp Neurol* **280**: 587-602.

Ju G, Swanson LW. 1989b. Studies on the cellular architecture of the bed nuclei of the stria terminalis in the rat: II. Chemoarchitecture. *J Comp Neurol* **280**: 603-621.

Kaada, BR. 1972. Stimulation and regional ablation of the amygdaloid complex with reference to functional representations. In: The Neurobiology of the Amygdala. Ed. B. E. Eleftheriou. Plenum Press: New York 205–282.

Kalin NH, Shelton SE. 1989. Defensive behaviors in infant rhesus monkeys: environmental cues and neurochemical regulation. *Science* **243**:1718–1721.

Kang W, Wilson MA, Bender MA, Glorioso JC, Wilson SP. 1998. Herpes virus-mediated preproenkephalin gene transfer to the amygdala is antinociceptive. *Brain Res* 792: 133–135.

Kapp BS, Frysinger RC, Gallagher M, Haselton JR. 1979. Amygdala central nucleus lesions: effect on heart rate conditioning in the rabbit. *Physiol Behav*

23:1109 –1117.

Kasckow JW, Baker D, Geracioti TD Jr. 2001. Corticotropin-releasing hormone in depression and post-traumatic stress disorder. *Peptides* **22**: 845–851.

Kellicut MH, Schwarzbaum JS. 1963. Formation of a conditioned emotional response (CER) following lesions of the amygdaloid complex in rats. Psychol Rev **12**: 351–358.

Killcross S, Robbins TW, Everitt BJ. 1997. Different types of fear-conditioned behaviour mediated by separate nuclei within amygdala. *Nature* **388**: 377–380.

Kim M, Campeau S, Falls WA, Davis M. 1993. Infusion of the non-NMDA receptor antagonist CNQX into the amygdala blocks the expression of fear-potentiated startle. *Behav Neural Biol* **59**: 5–8.

Kloosterman F, Davidson TJ, Gomperts SN, Layton SP, Hale G, Nguyen DP, Wilson MA. 2009. Micro-drive array for chronic in vivo recording: drive fabrication. *J Vis Exp* **20**: 26.

Kluver H, Bucy PC. 1937. “Psychic blindness” and other symptoms following bilateral temporal lobectomy in rhesus monkeys. *Am. J Physiol* **119**: 352-353.

Koo JW, Han JS, Kim JJ. 2004. Selective neurotoxic lesions of basolateral and central nuclei of the amygdala produce differential effects on fear conditioning. *J Neurosci* **24**: 7654-7662.

Krasne FB & Glanzman DL. 1995. What we can learn from invertebrate learning. *Ann Rev Psychol* **46**: 585-624.

Krawczyk M, Georges F, Sharma R, Mason X, Berthet A, Bézard E, Dumont EC. 2011. Double-dissociation of the catecholaminergic modulation of synaptic transmission in the oval bed nucleus of the stria terminalis. *J Neurophysiol* **105**: 145-53.

Krettek JE, Price JL. 1978a. Amygdaloid projections to subcortical structures within the basal forebrain and branstem of the rat and cat. *J Comp Neurol* **178**: 225-53.

Krettek JE, Price JL. 1979b. A description of the amygdaloid complex in the rat and cat with observations on intra-amygdaloid axonal connections. *J Comp Neurol* **178**: 255–280.

LeDoux JE, Iwata J, Pearl D, Reis DJ. 1986. Disruption of auditory but not visual learning by destruction of intrinsic neurons in the rat medial geniculate body. *Brain Res* **371**: 395–399.

LeDoux JE. 1987. Emotion. In: Plum F, editor. Handbook of Physiology. 1: The Nervous System. Vol V, Higher Functions of the Brain. Bethesda: American Physiological Society; 419–460.

LeDoux JE. 1998. The emotional brain. New York: Simon and Schuster pp: 384-8.

LeDoux JE, Iwata J, Cicchetti P, Reis DJ. 1988. Different projections of the central amygdaloid nucleus mediate autonomic and behavioral correlates of conditioned fear. *J Neurosci* **8**: 2517–2529.

LeDoux JE, Cicchetti P, Xagoraris A, Romanski LM. 1990a. The lateral amygdaloid nucleus: sensory interface of the amygdala in fear conditioning. *J Neurosci* **10**: 1062-9.

LeDoux JE. 2000. Emotion circuits in the brain. *Annu Rev Neurosci* **23**: 155–184.

Letzkus JJ, Wolff SB, Meyer EM, Tovote P, Courtin J, Herry C, Lüthi A. 2011. A disinhibitory microcircuit for associative fear learning in the auditory cortex. *Nature* **480**: 331-5.

Li CI, Maglinao TL, Takahashi LK. 2004. Medial amygdala modulation of predator odor-induced unconditioned fear in the rat. *Behav Neurosci* **118**: 324–332.

Lipski J. 1981. Antidromic activation of neurons as an analytic tool in the study of the central nervous system. *J Neurosci Methods* 2: 1-32.

Liu TL, Chen DY, Liang KC. 2009. Post-training infusion of glutamate into the bed nucleus of the stria terminalis enhanced inhibitory avoidance memory: an effect involving norepinephrine. *Neurobiol Learn Mem* **91**: 456-65.

Lu L, Hope BT, Dempsey J, Liu SY, Bossert JM, Shaham Y. 2005. Central amygdala ERK signalling pathway is critical to incubation of cocaine craving. *Nat Neurosci* **8**: 212–219.

Luppi A, Bucci G, Maini P, Rocourt J. 1988. Ecological survey of Listeria in the Ferrara area (northern Italy). *Zentralbl Bakteriol Mikrobiol Hyg A* **269**: 266-75.

Luyten L, van Kuyck K, Vansteenwegen D, Nuttin B. 2011. Electrolytic lesions of the bed nucleus of the stria terminalis disrupt freezing and startle potentiation in a conditioned context. *Behav Brain Res* **222**: 357-62.

MacLean PD, Delgado JM. 1953. Electrical and chemical stimulation of frontotemporal portion of limbic system in the waking animal. *Electro-encephalogr Clin Neurophysiol Suppl* **5**: 91–100.

Maier SF. 1990. Role of fear in mediating shuttle escape learning deficit produced by inescapable shock. *J Exp Psychol Anim Behav Process* **16**:137-49.

Marchilhac A, Siaud P. 1997. Identification of projections from the central nucleus of the amygdala to the paraventricular nucleus of the hypothalamus which are immunoreactive for corticotrophin- releasing hormone in the rat. *Exp Physiol* **82**: 273–281.

Maren S, De Oca B, Fanselow MS. 1994. Sex differences in hippocampal long-term potentiation (LTP) and Pavlovian fear conditioning in rats: positive correlation between LTP and contextual learning. *Brain Research* **661**: 25–34.

Maren S. 2001. Neurobiology of Pavlovian Fear Conditioning. *Annual Review of Neuroscience* **14**: 897-931.

Maren S, Quirk GJ. 2004. Neuronal signalling of fear memory. *Nat Rev Neurosci* **5**: 844–852.

Maren S. 2008. Pavlovian fear conditioning as a behavioral assay for hippocampus and amygdala function: cautions and caveats. *Eur J Neurosci* **28**:1661-6.

Mascagni F, McDonald AJ, Coleman JR. 1993. Corticoamygdaloid and corticocortical projections of the rat temporal cortex: A phaseolus vulgaris leucoagglutinin study. *Neuroscience* **57**: 697– 715.

McEwen BS, Stellar E. 1993. Stress and the individual: mechanisms leading to disease. *Arch Intern Med* **153**: 2093-2101.

McEwen BS, Sapolsky RM 1995. Stress and cognitive funciton. *Curr Opin Neurobiol* **5**: 205-16.

McEwen BS. 1998. Stress, adaptation, and disease. Allostasis and allostatic load. *Ann NY Acad Sci* **840**: 33–44.

McDonald AJ. 1982. Cytoarchitecture of the central amygdaloid nucleus of the rat. *J Comp Neurol* **208**: 401-418.

McDonald AJ. 1998. Cortical pathways to the mammalian amygdala. *Prog Neurobiol* **55**: 257-332.

McDonald AJ. 2003. Is there an amygdala and how far does it extend? An anatomical perspective. *Ann N Y Acad Sci* **985**: 1-21.

McGaugh JL. 2000. Memory--a century of consolidation. *Science* **287**: 248-251.

McGaugh JL, Roozendaal B. 2002. Role of adrenal stress hormones in forming lasting memories in the brain. *Curr Opin Neurobiol* **12**: 205-10.

McGaugh JL. 2004. The amygdala modulates the consolidation of memories of emotionally arousing experiences. *Annu Rev Neurosci* **27**: 1-28.

McLemore S, Crown ED, Meagher MW, Grau JW. 1999. Shock-induced hyperalgesia: II. Role of the dorsolateral periaqueductal gray. *Behav Neurosci* **113**: 539–549.

Meloni EG, Jackson A, Gerety LP, Cohen BM, Carlezon WA Jr. 2006. Role of the bed nucleus of the stria terminalis (BST) in the expression of conditioned fear. *Ann N Y Acad Sci* **1071**: 538-41.

McElligott ZA, Winder DG. 2009. Modulation of glutamatergic synaptic transmission in the bed nucleus of the stria terminalis. *Prog Neuropsychopharmacol Biol Psychiatry* **33**:1329-35.

Moga MM, Saper CB, Gray TS. 1989. Bed nucleus of the stria terminalis: cytoarchitecture, immunohistochemistry, and projection to the parabrachial nucleus in the rat. *J Comp Neurol* **283**: 315-32.

Paré D. 2003. Role of the basolateral amygdala in memory consolidation. *Prog Neurobiol* **70**: 409-420.

Medina JF, Repa JC, Mauk MD, LeDoux JE. 2002. Parallels between cerebellum- and Amygdala-Dependant conditioning. *Nature Reviews Neuroscience* **3**: 122-131.

Miserendino MJ, Sananes CB, Melia KR, Davis M. 1990. Blocking of acquisition but not expression of conditioned fear-potentiated startle by NMDA antagonists in the amygdala. *Nature* **345**:716–718.

Muller M, Fendt M. 2006. Temporary inactivation of the medial and basolateral amygdala differentially affects TMT-induced fear behavior in rats. *Behav Brain Res* **167**: 57–62.

Nagy FZ, Paré D. 2008. Timing of Impulses from the central amygdala and bed nucleus of the stria terminalis to the brain stem. *J Neurophys* **100**: 3429-3436.

Pacak K, Palkovits M, Kopin IJ, Goldstein DS. 1995. Stress-induced norepinephrine release in the hypothalamic paraventricular nucleus and pituitary-adrenocortical and sympathoadrenal activity: In vivo microdialysis studies. *Front Neuroendocrinol* **16**: 89-150.

Packard MG, Cahill L, McGaugh JL. 1994. Amygdala modulation of hippocampal-dependent and caudate nucleus-dependent memory processes.

Proc Natl Acad Sci USA **91**: 8477–8481.

Pape HC, Paré D. 2010. Plastic synaptic networks of the amygdala for the acquisition, expression, and extinction of conditioned fear. *Physiol Rev* **90**: 419-63.

Paré D, Smith Y. 1993. The intercalated cell masses project to the central and medial nuclei of the amygdala in cats. *Neuroscience* **57**: 1077–1090.

Paré D, Smith Y, and Paré JF. 1995. Intra-amygdaloid projections of the basolateral and basomedial nuclei in the cat: Phaseolus vulgaris-leucoagglutinin anterograde tracing at the light and electronmicroscopic level. *Neuroscience* **69**: 567–583.

Paré D, Quirk GJ, Ledoux JE. 2004. New vistas on amygdala networks in conditioned fear. *J Neurophysiol* **92**: 1-9.

Paré D, Duvarci S. 2012. Amygdala microcircuits mediating fear expression and extinction. *Current Opinion in Neurobiology* **22**: 717–723.

Pascoe JP, Kapp BS. 1985. Electrophysiological characteristics of amygdaloid central nucleus neurons in the awake rabbit. *Brain Res Bull* **14**: 331-8.

Pavlov IP, Anrep GV. 1927. Conditioned Reflexes; An Investigation of the Physiological Activity of the Cerebral Cortex. Oxford University Press/Humphrey, Milford, London.

Petrovich GD, Swanson LW. 1997. Projections from the lateral part of the central amygdala nucleus to the postulated fear conditioning circuit. *Brain Res* **763**: 247-54.

Pitkänen A, Stefanacci L, Far CR, Go GG, LeDoux JE, Amaral DG. 1995. Intrinsic connections of the rat amygdaloid complex: projections originating in the lateral nucleus. *J Comp Neurol* **356**: 288-310.

Pitkänen A, Savander V, LeDoux JE. 1997. Organization of intra-amygdaloid circuitries in the rat: an emerging framework for understanding functions of the amygdala. *Trends Neurosci* **20**: 517-23.

Pitts MW, Todorovic C, Blank T, Takahashi LK. 2009. The central nucleus of the amygdala and corticotropin-releasing factor: insights into contextual fear memory. *J Neurosci* **29**: 7379-88.

Poulin JF, Chevalier B, Laforest S, Drolet G. 2006. Enkephalinergic afferents of the centromedial amygdala in the rat. *J Comp Neurol* **496**: 859-76.

Prewitt CM, Herman JP. 1998. Anatomical interactions between the central amygdaloid nucleus and the hypothalamic paraventricular nucleus of the rat: a dual tract-tracing analysis. *J Chem Neuroanat* **15**: 173–185.

Price JL, Amaral DG. 1981. An autoradiographic study of the projections of the central nucleus of the monkey amygdala. *J Neurosci* 1: 1242–1259.

Quirk GJ. 2002. Memory for extinction of conditioned fear is long-lasting and persists following spontaneous recovery. *Learn Mem* **9**: 402–407.

Quirk GJ, Likhtik E, Pelletier JG, Paré D. 2003. Stimulation of medial prefrontal cortex decreases the responsiveness of central amygdala output neurons. *J Neurosci* 23: 8800-7.

Quirk GJ, Beer JS. 2006. Prefrontal involvement in the regulation of emotion: convergence of rat and human studies. *Curr Opin Neurobiol* 16: 723–727.

Raybuck JD, Lattal KM. 2011. Double dissociation of amygdala and hippocampal contributions to trace and delay fear conditioning. *PLoS One* **6**: e15982.

Rechtschaffen A. 1998. Current perspectives on the function of sleep. *Perspect Biol Med* **41**: 359-90.

Rescorla RA. 1968. Probability of shock in the presence and absence of CS in fear conditioning. *J Comp Physiol Psychol* **66**: 1–5.

Rescorla RA**.** 2001. Retraining of extinguished Pavlovian stimuli. *J Exp Psychol Anim Behav Process* **27**: 115–124.

Resstel LB, Alves FH, Reis DG, Crestani CC, Correa FM, Guimaraes FS. 2008. Anxiolytic-like effects induced by acute reversible inactivation of the bed nucleus of stria terminalis. *Neuroscience* **154**: 860-76.

Rizvi TA, Ennis M, Behbehani MM, Shipley MT. 1991. Connections between the central nucleus of the amygdala and the midbrain periaqueductal gray: topography and reciprocity. *J Comp Neurol* **303**: 121-131.

Rogan MT, LeDoux JE. 1996. Emotion: systems, cells, synaptic plasticity. *Cell* **85**: 469-75.

Rogan MT, Staubli UV, Ledoux JE. 1997. Fear conditioning induces associative long-term potentiation in the amygdala. *Nature* **390**: 604–607.

Romanski LM, LeDoux JE. 1992. Equipotentiality of thalamo-amygdala and

thalamo-cortico- amygdala circuits in auditory fear conditioning. *J Neurosci* **12**: 4501–4509.

Royer S, Martina M, Paré D. 1999. An inhibitory interface gates impulse traffic between the input and output stations of the amygdala. *J Neurosci* **19**: 10575-83.

Sah P, Faber ES, Lopez De Armentia M, Power J. 2003. The amygdaloid complex: anatomy and physiology. *Physiol Rev* **83**: 803-34.

Saha S. 2005. Role of the central nucleus of the amygdala in the control of blood pressure: descending pathways to medullary cardiovascular nuclei. *Clin Exp Pharmacol Physiol* **32**: 450-6.

Savander V, Go CG, LeDoux JE, Pitkänen A. 1995. Intrinsic connections of the rat amygdaloid complex: Projections originating in the basal nucleus. *J Comp Neurol* **361:** 345-368.

Sawchenko PE, Swanson LW. 1983. The organization of forebrain afferents to the paraventricular and supraoptic nuclei of the rat. *J Comp Neurol* **218**: 121–144.

Schafe GE, Nader K, Blair HT, Ledoux JE. 2001. Memory consolidation of Pavlovian fear conditioning: a cellular and molecular perspective. *TINS* **24**: 540–546.

Schwaber JS, Kapp BS, Higgins GA, Rapp PR. 1982. Amygdaloid and basal forebrain direct connections with the nucleus of the solitary tract and the dorsal motor nucleus. *J Neurosci* 2: 1424-38.

Shin JW, Geerling JC, Loewy AD. 2008. Inputs to the ventrolateral bed nucleus of the stria terminalis. *J Comp Neurol* **511**: 628-57.

Shipley MT, Ennis M, Puche A. 2004. Olfactory system. In: Paxinos, G. (Ed.), The Rat Nervous System. Elsevier Academic Press, San Diego, pp. 923–964.

Siapas AG, Wilson MA. 1998. Coordinated Interactions between Hippocampal Ripples and Cortical Spindles during Slow-Wave Sleep. *Neuron* **21**: 1123–1128.

Simerly RB. 2002. Wired for reproduction: organization and development of sexually dimorphic circuits in the mammalian forebrain. *Annu Rev Neurosci* **25**: 507-36.

Sink KS, Walker DL, Yang Y, Davis M. 2011. Calcitonin gene-related peptide in

the bed nucleus of the stria terminalis produces an anxiety-like pattern of behavior and increases neural activation in anxiety-related structures. *J Neurosci* **31:** 1802-10.

Smith BS**,** Millhouse OE. 1985. The connections between the basolateral and central amygdaloid nuclei. *Neurosci Lett* **56**: 307–309.

Sofroniew MV. 1983. Direct reciprocal connections between the bed nucleus of the stria terminalis and dorsomedial medulla oblongata: evidence from immunohistochemical detection of tracer proteins. *J Comp Neurol* **213**: 399-405.

Steriade M, Hobson J. 1976. Neuronal activity during the sleep-waking cycle. *Prog Neurobiol* **6**:155-376.

Steriade M. 1997. Synchronized activities of coupled oscillators in the cerebral cortex and thalamus at different levels of vigilance. *Cereb Cortex* **7**: 583-604.

Sullivan GM, Apergis J, Bush DE, Johnson LR, Hou M, Ledoux JE. 2004. Lesions in the bed nucleus of the stria terminalis disrupt corticosterone and freezing responses elicited by a contextual but not by a specific cue-conditioned fear stimulus. *Neuroscience* **128**: 7-14.

Sun N, Roberts L, Cassell MD. 1991. Rat central amygdaloid nucleus projections to the bed nucleus of the stria terminalis. Brain Res Bull **27**: 651-62.

Sun N, Cassell MD. 1993. Intrinsic GABAergic neurons in the rat central extended amygdala. *J Comp Neurol* **330**: 381-404.

Sun N, Yi H, Cassell MD. 1994. Evidence for a GABAergic interface between cortical afferents and brainstem projection neurons in the rat central extended amygdala. *J Comp Neurol* **340**: 43-64.

Takayama, K., Okada, J. & Miura, M. 1990. Evidence that neurons of the central amygdaloid nucleus directly project to the site concerned with circulatory and respiratory regulation in the ventrolateral nucleus of the cat: a WGA-HRP study. *Neurosci. Lett* **109**: 241–246.

Terreberry RR, Oguri M, Harper RM. 1995. State-dependent respiratory and cardiac relationships with neuronal discharge in the bed nucleus of the stria terminalis. *Sleep* **18**: 139-44.

Trei D, Pesold C, Rotzinger S. 1993. Dissociating the anti-fear effects of septal and amygdaloid lesions using two pharmacologically validated models of rat anxiety. *Behavioral Neuroscience* **107**: 770-785.

Van de Kar LD, Piechowski RA, Rittenhouse PA, Gray TS. 1991. Amygdaloid lesions: differential effect on conditioned stress and immobilization-induced increases in corticosterone and renin secretion. *Neuroendocrinology* **54**: 89–95.

Veening JG, Swanson LW, Sawchenko PE. 1984. The organization of projections from the central nucleus of the amygdala to brainstem sites involved in central autonomic regulation: a combined retrograde transport-immunohistochemical study. *Brain Res* **303**: 337–357.

Veinante P, Freund-Mercier M-J. 2003. Branching patterns of central amygdaloid nucleus efferents in the rat: single-axon reconstructions. *Ann NY Acad Sci* **985**: 552–553.

Vertes RP**.** 2004. Differential projections of the infralimbic and prelimbic cortex in the rat. *Synapse* **51**: 32–58.

Waddell J, Morris RW, Bouton ME. 2006. Effects of bed nucleus of the stria terminalis lesions on conditioned anxiety: Aversive conditioning with long-duration conditional stimuli and reinstatement of extinguished fear. *Behavioral Neuroscience* **120**: 324–336.

Walker DL, Davis M. 1997. Anxiogenic effects of high illumination levels assessed with the acoustic startle paradigm. *Biol Psy* **42**: 461–471.

Walker DL, Toufexis DJ, Davis M. 2003. Role of the bed nucleus of the stria terminalis versus the amygdala in fear, stress, and anxiety. *Eur J Pharmacol* **463**: 199 –216.

Walker DL, Miles LA, Davis M. 2009. Selective participation of the bed nucleus of the stria terminalis and CRF in sustained anxiety-like versus phasic fear-like responses. *Prog Neuropsychopharmacol Biol Psychiatry* **33:** 1291-308.

Wallace KJ, Rosen JB. 2001. Neurotoxic lesions of the lateral nucleus of the amygdala decrease conditioned fear but not unconditioned fear of a predator odor: comparison with electrolytic lesions. *J Neurosci* **21**: 3619–3627.

Whalen PJ, Phelps EA. 2009. The Human Amygdala, Guilford Press.

Weiskrantz L. 1956. Behavioral changes associated with ablation of the amygdaloid complex in monkeys. *J Comp Physiol Psychol* **49**: 391-91.

Weller KL, Smith DA. 1982).Afferent connections to the bed nucleus of the stria terminalis. *Brain Res* **232**: 255-70.

Wilensky AE, Schafe GE, Kristensen MP, LeDoux JE. 2006. Rethinking the fear circuit: the central nucleus of the amygdala is required for the acquisition,

consolidation, and expression of Pavlovian fear conditioning. *J Neurosci* **26**: 12387–12396.

Will MJ, Franzblau EB, Kelley AE. 2004. The amygdala is critical for opioid-mediated binge eating of fat. *Neuroreport* **15**: 1857–1860.

Wilson A, Kapp BS. 1994. Effect of lesions of the ventrolateral periaqueductal gray on the Pavlovian conditioned heart rate response in the rabbit. *Behav Neural Biol* **62**: 73–76.

Yajeya J, Criado Gutierrez J, Fernandez de Molina A. 1989. Unitary activity in the bed nucleus of the stria terminalis after homo- and contralateral stria terminalis stimulation. *Acta Physiol Scand*. **135**: 241-8.

Zimmerman JM, Maren S. 2011. The bed nucleus of the stria terminalis is required for the expression of contextual but not auditory freezing in rats with basolateral amygdala lesions. *Neurobiology of Learning and Memory* **95**: 199-205.

Zhang JX, Harper RM, Frysinger RC. 1986. Respiratory modulation of neuronal discharge in the central nucleus of the amygdala during sleep and waking states. *J Exp Neurol* **91**: 193-207.

VITA

Frank Nagy

1976 Born March 23rd in New York, New York

1994 Graduated from Northern Valley Regional High School, Demarest, NJ. 1994-98 Attended Semmelweis University Of Medicine, Budapest, HU.

2002 Graduated from Drew University, Madison, NJ BA Economics.

2001-02 Research Assistant, UMDNJ, Newark, NJ.

2002-13 Doctoral work at Rutgers University.

2013 PhD in Behavioral and Neural Sciences, Rutgers U., Newark, NJ.

2000 Article: Receptor subtypes mediating depressor responses to microinjections of nicotine into medial NTS of rat. Am J Physiol Regul Integr Comp Physiol. Jul; 279(1):R132-40.

2008 Article: Timing of impulses from the central amygdala and bed nucleus of the stria terminalis to the brain stem. J Neurophysiol. 2008 Dec;100(6):3429-36.

2010 Article: Facilitation of corticostriatal plasticity by the amygdala requires Ca2+-induced Ca2+ release in the ventral striatum. J Neurophysiol. 2010 Sep;104(3):1673-80.

2013 Article: Neuronal correlates of fear conditioning in the bed nucleus of the stria terminalis. Learning and Memory. In press.